Received: 27 February 2024 | Accepted: 13 April 2024

DOI: 10.1002/jmv.29630

RESEARCH ARTICLE

JOURNAL OF MEDICAL VIROLOGY WILEY

Dual T cell receptor/chimeric antigen receptor engineered NK-92 cells targeting the HPV16 E6 oncoprotein and the tumor-associated antigen L1CAM exhibit enhanced cytotoxicity and specificity against tumor cells

Isaac Quiros-Fernandez[1,2] | Sofia Libório-Ramos[1] | Lena Leifert[1] | Bruno Schönfelder[1] | Israel Vlodavsky[3] | Angel Cid-Arregui[1]

[1]Targeted Tumor Vaccines Group, Clinical Cooperation Unit Applied Tumor Immunity, German Cancer Research Center (DKFZ), Heidelberg, Germany

[2]Research Center on Tropical Diseases (CIET)/ Research Center on Surgery and Cancer (CICICA), Faculty of Microbiology, Universidad de Costa Rica, San Jose, Costa Rica

[3]Technion Integrated Cancer Center (TICC), Rappaport Faculty of Medicine, Technion - Israel Institute of Technology, Haifa, Israel

Correspondence

Angel Cid-Arregui, Targeted Tumor Vaccines Group, Clinical Cooperation Unit Applied Tumor Immunity, German Cancer Research Center (DKFZ), Heidelberg, Germany.
Email: a.cid@dkfz-heidelberg.de

Funding information

University of Costa Rica and the German DAAD; Cooperation Program in Cancer Research of the Deutsches Krebsforschungszentrum (DKFZ) and Israel's Ministry of Science, Technology and Space (MOST)

Abstract

The human papillomavirus type 16 (HPV16) causes a large fraction of genital and oropharyngeal carcinomas. To maintain the transformed state, the tumor cells must continuously synthesize the E6 and E7 viral oncoproteins, which makes them tumor-specific antigens. Indeed, specific T cell responses against them have been well documented and $CD8^+$ T cells engineered to express T cell receptors (TCRs) that recognize epitopes of E6 or E7 have been tested in clinical studies with promising results, yet with limited clinical success. Using $CD8^+$ T cells from peripheral blood of healthy donors, we have identified two novel TCRs reactive to an unexplored $E6_{18\text{-}26}$ epitope. These TCRs showed limited standalone cytotoxicity against $E6_{18\text{-}26}$-HLA-A*02:01-presenting tumor cells. However, a single-signaling domain chimeric antigen receptor (ssdCAR) targeting L1CAM, a cell adhesion protein frequently overexpressed in HPV16-induced cancer, prompted a synergistic effect that significantly enhanced the cytotoxic capacity of NK-92/CD3/CD8 cells armored with both TCR and ssdCAR when both receptors simultaneously engaged their respective targets, as shown by live microscopy of 2-D and 3-D co-cultures. Thus, virus-specific TCRs from the $CD8^+$ T cell repertoire of healthy donors can be combined with a suitable ssdCAR to enhance the cytotoxic capacity of the effector cells and, indirectly, their specificity.

KEYWORDS

adoptive cell transfer, CAR, cell therapy, cervical cancer, chimeric antigen receptor, human papillomavirus, immunotherapy, T cell receptor

1 | INTRODUCTION

Clinical studies on immunotherapy of solid tumors using T cell receptor (TCR)–engineered immune cells (e.g., NK or T cells) targeting tumor antigens are providing exciting data (reviewed in.[1] Indeed, TCR-based immune cell therapy offers important advantages over chimeric antigen receptor (CAR) immunotherapy, such as wider repertoire of targetable (surface and intracellular) tumor antigens; higher sensitivity (target epitope densities required for signaling are 2–3 orders of magnitude lower); and lower affinity of TCRs for their target compared to CARs, but higher avidity of TCR T cells that enables them to eliminate several tumor cells sequentially.[2]

The human papillomavirus type 16 (HPV16) is a main causative agent of cervical, anogenital and oropharyngeal cancers. Two viral oncogenes, E6 and E7, have been extensively characterized as the major oncogenic drivers (reviewed in Ref[3]). By interacting with a variety of cellular proteins, E6 and E7 synergize in promoting unregulated cellular proliferation.[4,5] Continuous expression of both viral oncoproteins is required to maintain the transformed phenotype of HPV16-infected cancer cells. Hence, they represent attractive tumor-specific targets for adoptive T cell therapies. In particular, the E6 protein has been implicated in the proteasome-mediated degradation of p53, promotion of telomerase expression and inhibition of innate immune responses. Silencing of the E6 gene in HPV16-transformed cells, leads to apoptosis [6,7] emphasizing the E6 protein as an ideal immunotherapy target. The $E6_{18\text{-}26}$ peptide was the first E6 epitope recognized. It was identified by sequential Edman degradation of peptides from the HLA-A*02:01+ cell line JY infected with a recombinant Vaccinia virus expressing a HPV16 E6 gene.[8] Surprisingly, immunopeptidomics analyses carried out years later with the CaSki HPV16$^+$ cervical cancer cell line failed to detect the $E6_{18\text{-}26}$ peptide but not the $E6_{29^-38}$ peptide. However, the signal obtained from mass spectrometry was close to the limit of detection.[9] Later, a TCR reactive to the $E6_{29\text{-}38}$ peptide was identified from tumor infiltrating lymphocytes (TILs) of a cancer patient and tested in a phase I/II clinical trial,[10] albeit with limited success, with just two out of twelve patients showing partial responses.[11] No further clinical trials have been reported to date with the $E6_{29\text{-}38}$ TCR. More recently, however, deep sequencing studies have identified several E6 variants in patients with high-grade squamous intraepithelial lesions (HSIL) caused by HPV16, with a hotspot located at codon 32.[12] The most prevalent was the D32E variant, which was shown to have an enhanced capacity to promote TP53 degradation. This mutation also changes the conformation of the $E6_{29\text{-}38}$ epitope, which might then not be recognized by the TCR, leading to failure of the immunotherapy in the clinical trial. Thus, there is an unmet need for improvement of the efficacy of treatments based on TCR-engineered immune cells against HPV16 antigens.

Taking into consideration the previous experience, we decided to identify new TCRs that recognize the $E6_{18\text{-}26}$ epitope and to enhance the signaling strength and functionality of immune effector cells after engagement of the TCR with the peptide-HLA complex through a dual strategy combining, in the same immune cell, the TCR and a new chimeric antigen receptor (CAR) against L1CAM (L1 cell adhesion molecule), which is frequently overexpressed in cancers caused by HPV16. We have previously reported a strategy to enhance the cytotoxic capacity of TCR-engineered effector cells by utilizing a costimulatory CAR targeting a tumor-associated surface protein,[13] now we have aimed to follow a similar approach by targeting L1CAM with a milder CAR carrying just one signaling domain. L1CAM is a neural cell adhesion molecule that is involved in the development of the central nervous system, in axon guidance, neural cell migration and differentiation.[14] Nevertheless, L1CAM has been found over-expressed in many types of tumors and its expression correlates with disease stage, progression and aggressiveness.[15–18] In cervical and oral squamous cell carcinomas caused by HPV16, L1CAM is a strong predictor for recurrence and decreased survival,[19,20] besides, L1CAM expression is associated with larger and more aggressive tumors and lower disease-free and overall survival.[21]

In this work, we report the identification of novel TCRs reactive against the HPV16 $E6_{18\text{-}26}$ epitope in the context of HLA-A*02:01. Additionally, we have validated the combination in the same effector NK cell of an E6-TCR and a single-signaling domain chimeric antigen receptor (ssdCAR) directed against L1CAM, engineered to have a unique activating domain in its intracellular tail incapable of providing standalone activation upon binding to L1CAM. Our results demonstrate that, the HPV16 $E6_{18\text{-}26}$ peptide is indeed presented by HPV16$^+$ and HLA-A*02:01$^+$ cervical cancer and head and neck carcinoma cell lines. Further, NK-92 cells expressing both a TCR recognizing HPV16 $E6_{18\text{-}26}$ and a L1CAM directed ssdCAR are capable of improved TCR-mediated cytotoxicity in an antigen-specific manner.

2 | MATERIALS AND METHODS

2.1 | In silico prediction of epitopes from the HPV16 E6 protein presented in the context of HLA-A*02:01

The amino acid sequence of the HPV16 E6 protein was retrieved from the UniProt database (Accession number P03126). The E6 sequence was loaded on the NetCTLPan neural network model from the Immune Epitope Database and Analysis Resource.[22] This model offers the possibility of predicting simultaneously scores for proteasome degradation, TAP processing and HLA binding of a protein for a specific HLA type. The HLA-A*02:01 was selected and the prediction of putative epitopes was performed for peptide lengths of 9, 10 and 11 amino acids.

2.2 | Cell lines, culture conditions, electroporation and immunostaining

The cervical cancer cell lines CaSki, SiHa, and C33a and the head and neck squamous cell carcinoma (HNSCC) cell lines UPCI-SCC-154 and

PCI-13 were cultured in DMEM (Gibco) supplemented with 10% fetal bovine serum (FBS, Gibco) and penicillin/streptomycin. The Jurkat J76/CD8 [23] and the T2 [24] cell lines were cultured in RPMI-1640 (Gibco) supplemented with 10% FBS and penicillin/streptomycin (Gibco). The NK-92CI cell line [25] was cultured in X-Vivo™20 (Lonza) supplemented with 5% FBS. Primary CD8 T cells were cultured in X-Vivo™20 (Lonza) supplemented with 10% FBS, interleukin 2 (IL-2, Peprotech, 100 UI/mL), IL-7 (Biolegend, 10 ng/mL) and IL-15 (Peprotech, 10 ng/mL), unless stated otherwise. All cell lines and primary cells were cultured at 37°C and 5% CO_2. The cancer cell lines used in this study were tested for L1CAM expression by antibody staining. Cells (1×10^5) were washed with five volumes of FACS buffer and stained using anti-L1CAM-PE (RRID AB_2616787) or isotype control antibodies for 30 min on ice. Then the cells were washed with 10 volumes of FACS buffer, and finally resuspended in FACS buffer containing DAPI (0.5 µg/mL). Dead cells were excluded by gating DAPI-negative cells.

For the analysis of expression of ICOS in the NK-92 cell line, cells (1×10^5) were washed with five volumes of FACS buffer and stained with either anti-human-ICOS-PE (RRID AB_416331 or an isotype control for 30 min on ice. Then the cells were washed with 10 volumes of FACS buffer and resuspended in FACS buffer containing DAPI (0.5 µg/mL). Dead cells were excluded with DAPI. Flow cytometry measurements was performed in a BD FACSCanto™ II.

2.3 | Generation of cervical/head and neck cancer cell lines with stable expression of HLA-A*02:01 or mWasabi fluorescent protein

To produce cervical and HNSCC cell lines stably expressing either HLA-A*02:01 or the mWasabi fluorescent protein, synthetic genes encoding the human HLA-A*02:01 and beta-2-microglobulin (β2M) or the mWasabi proteins [26] were cloned in the pSBbi-Pur. The cells (1×10^6) were washed with PBS twice and resuspended in 20 µL of SE Nucleofector solution (Lonza) containing 1 µL of DNA mix (0.6 µg pSB and 0.4 µg of pCMV-SB100X). The cells were electroporated immediately after adding the plasmid in a well of the SE Cell Line 4D-NucleofectorTM X Kit S (Lonza) using the program CA163. Then, the electroporated cells were incubated at room temperature for 10 min and transferred to a 48-well plate with 1 mL of culture medium. After 2 weeks in culture, the expanded cells were sorted based on staining with anti-human-HLA-A*02-APC antibody (RRID AB_2561567), 1 µg/mL final staining concentration, or mWasabi expression, using a BD FACSAria™ Fusion.

2.4 | Amplification and sequencing of E6 in HPV16$^+$ cancer cell lines

CaSki, SiHa or UPCI-SCC-154 cells were retrieved (0.5×10^6 cells) and washed twice with PBS. To prepare total cellular RNA, the RNeasy Mini Kit (Qiagen) RNA extraction was used. The extracted RNA was immediately used for reverse transcription using the RevertAid First Strand cDNA Synthesis Kit (Thermo Fisher) 1 h at 42°C with the Oligo(dT) 18 primer. The HPV16 E6 gene was amplified from the respective cDNAs using forward 5′–atgcaccaaaagagaactgca–3′ and reverse 5′–ttacagctgggtttctctacg–3′ primers (Sigma). To conduct the PCR, 25 µL of Phusion™ High Fidelity PCR Master Mix (2×) (Thermo Fisher) were mixed with 2.5 µL of cDNA, 2.5 µL forward primer (10 µM), 2.5 µL reverse primer (10 µM) and 12.5 µL of PCR-grade water. A three-step PCR was performed as follows: 98°C/30 s, followed by 35 cycles of [98°C/10 s; 60°C/10 s. 72°C/15 s], ending with 72°C/5 min. Finally, the amplified E6 genes were sequenced with the primers used for PCR amplification. The sequences obtained were translated and compared with the reference protein sequence of the HPV16 E6 protein (UniProt accession number P03126).

2.5 | Peptides and peptide-loaded-HLA-A*02:01$^-$multimers

The HPV16 $E6_{18\text{-}26}$ ($E6Q21H_{18\text{-}26}$ and $E6Q21D_{18\text{-}26}$), CMV $pp65_{495\text{-}503}$, and $Insulin_{34\text{-}42}$ peptides were obtained from ProteoGenix (Strasbourg, France) with a purity >95%. The peptides were dissolved in DMSO to a concentration of 20 mM and stored in aliquots at −80°C. HLA-A*02:01 multimers were prepared using Flex-T™ HLA-A*02:01 UVX monomers (Biolegend) following the protocol supplied by the manufacturer to conduct the peptide exchange by UV radiation. In brief, 20 µL of the HLA-A*02:01 UVX monomer were mixed with 20 µL of the peptide diluted to 400 µM in PBS. Then, the mixture was UV irradiated (366 nm) for 30 min, as recommended by the manufacturer. The irradiated solutions were immediately incubated at 37°C for additional 30 min. The efficiency of peptide exchange was measured by enzyme-linked immunosorbent assay (ELISA) using 2 µL of the reaction, the remainder reaction volume was divided in two parts and mixed with either APC-streptavidin (Biolegend) or PE-streptavidin (Biolegend) to generate two types of tetramers labeled with the respective fluorophores. Finally, D-biotin was added to the multimer solutions to block any remaining free streptavidin. The tetramers were always prepared the day before of the staining, and kept at 4°C in the dark overnight.

2.6 | Isolation of HPV16 $E6_{18\text{-}26}$$^-$reactive CD8$^+$ T cells

CD8$^+$ T cells were isolated from peripheral blood mononuclear cells (PBMCs). Peripheral blood samples were obtained from the Blood Banking facilities (Institut für Klinische Transfusionsmedizin und Zelltherapie Heidelberg, IKTZ, gGmbH) from healthy donors who signed informed consent for their blood being used anonymized for scientific research. First, it was diluted 1:2 with phosphate-buffered saline (PBS, Gibco) with 2 mM Ethylenediaminetetraacetic acid (EDTA, Thermo Scientific, 2 mM) and then centrifuged over Ficoll® Paque Plus (GE Healthcare) following the protocol recommended by

the provider. The buffy coats were washed twice (200×*g*, 10 min) to remove platelets from the preparation. The PBMCs were then counted and frozen in 50×10^6 cell aliquots in FBS with 10% dimethyl sulfoxide (DMSO, Thermo Scientific) and stored in liquid nitrogen. A small aliquot of the cells was taken before freezing for staining with the anti-HLA-A*02 antibody (RRID AB_2561567, 1 µg/mL as final staining concentration).

$CD8^+$ T cells from 10 different HLA-A*02^+ healthy donors were isolated using the human CD8 T cell isolation kit (Miltenyi Biotec). The CD8 T cells from each donor were maintained in separate wells of a 24-well-plate with 2 mL of medium per well. On the following day, the CD8 T cells were pooled together and the tetramer staining was carried out. The pooled CD8 T cells were washed twice with fluorescence-activated cell sorting (FACS) buffer (PBS and 0.5% bovine serum albumin fraction V, Merck). Next the cells were resuspended in FACS buffer and incubated on ice for 30 min with the respective HPV16 $E6_{18\text{-}26}$-HLA-A*02:01 tetramers (PE- or APC-labeled) at a final concentration of 1 µg/mL of each tetramer in 100 µL per 10^6 CD8 T cells. Then, an equal volume of FACS buffer with anti-CD8 FITC (RRID AB_1877178) and anti-CD3 PE-Cy7 (RRID AB_2561452) antibodies was added to the sample, mixed and further incubated under the same conditions for 15 min. Next, the sample was washed three times with five volumes of FACS Buffer, then, the cells were resuspended in 3 mL of FACS buffer containing 0.5 µg/mL DAPI (Thermo Fisher Scientific). $CD3^+/CD8^+$ T cells that were double positive for the HLA-A*02:01 tetramers were gated and sorted using a BD FACSAria™ Fusion and immediately centrifuged and resuspended in 150 µL of XVIVO20 with 10% FBS supplemented with IL-2 (1000 UI/mL) and 1 µL of T Cell TransAct™ (Miltenyi Biotec), transferred to a well of a U-bottom 96-well-plate and incubated at 37°C/5% CO2 for 2 weeks replacing the medium with fresh medium as required. Subsequently, the cells were retrieved and stained with the labeled tetramers and antibodies as above. Then, double positive cells for PE- and APC-HLA-A*02:01 tetramers were subjected to single-cell sorting in 96-well non-skirted PCR plates (Thermo Fisher Scientific) containing 11 µL/well of PCR-grade water. Finally, the 96-well plate was sealed, centrifuged for 1 min at 200xg, and kept frozen at −80°C until needed.

2.7 | Amplification and cloning of *TRAV* and *TRBV* from single $CD8^+$ T cells

Antigen-specific CD8 T cells previously sorted in a 96-well PCR plate with 11 µL of PCR-grade water per well were thawed and used for reverse transcription using the RevertAid First Strand cDNA Synthesis Kit (Thermo Fisher Scientific). In brief, 1 µL of RiboLock RNase Inhibitor (20 U/µL) and 1 µL of Oligo (dT)18 primer were added to each well. Then, the samples were incubated for 4 min at 70°C and subsequently for additional 4 min at 42°C to facilitate the lysis of the cells and annealing of the primers to poly(A)$^+$ mRNA. Then, 4 µL of reaction buffer (5×), 2 µL of 10 mM dNTP Mix and 1 µL RevertAid M-MuLV Reverse Transcriptase (200 U/µL) were added. The reaction was gently vortexed, spun down, and incubated for 1 h at 42°C for the cDNA synthesis to take place, and 10 min at 70°C for enzyme inactivation. To identify paired TRAV and TRBV from each sorted cell, the cDNAs of each well were used for two separate nested PCRs. First, aliquots of 2.5 µL of each cDNA preparation were used for a multiplex PCR amplification using two sets of external forward primers covering all TRAV and TRBV genes, which were validated previously [18] for TRAV and TRBV, and an external reverse TRAC or TRBC primer, respectively, to final concentrations of 400 nM. For the first PCR, 12.5 µL of Phusion™ High Fidelity PCR Master Mix (2×) were mixed with 2.5 µL of cDNA and 10 µL of external primer mix. The PCR conditions were 98°C/30 s, followed by 25 cycles at [98°C/10 s; 60°C/10 s; 72°C/15 s], ending with 72°C/5 min. For the second PCR, 1 µL of the first PCR reaction was mixed with 12.5 µL of Thermo Scientific™ Phusion™ High Fidelity PCR Master Mix (2×) and 11.5 µL of internal primer mix (each primer to a final concentration of 400 nM). The PCR conditions were 98°C/30 s, followed by 35 cycles at [98°C/10 s; 61°C/10 s; 72°C/15 s], ending with 72°C/5 min. The reaction products were separated in a 1.2% agarose gel. For each single cell TRAV and TRBV fragments in the range of 200–400 bp were purified using a Gel Extraction Kit (Qiagen) and Sanger sequenced using the respective TRAC or TRBC internal primer. Sequencing results were analyzed with the IMGT/V-QUEST online tool to identify the TRAV and TRBV genes and the complementarity determining region 3 (CDR3).[27] We used synthetic gene fragments of paired alpha and beta variable fragments (synthesized by Twist Bioscience) to construct each TCR following the order: [variable beta chain–murine constant beta chain–GSG–T2A–variable alpha chain–murine constant alpha chain]. The fragments were sequentially inserted in the Sleeping Beauty plasmid pSBbi-Pur (pSBbi-Pur-TCR), a gift from Eric Kowarz (RRID Addgene_60523),[28] using ClaI and SpeI (for the beta variable fragment) and; XmaI and NcoI (for the alpha variable fragment).

2.8 | Electroporation of Jurkat J76/CD8 cells for stable expression of murinized TCRs and tetramer staining

Jurkat J76/CD8 cells [29] (2×10^6 cells) were washed with PBS twice and resuspended in 20 µL of SE Nucleofector solution (Lonza) containing 1 µL of DNA mix (0.6 µg pSB-TCR and 0.4 µg of pCMV-SB100X). The cells were electroporated immediately after adding the plasmid using the SE Cell Line 4D-NucleofectorTM X Kit S (Lonza) using the program CL120. Then, the electroporated cells were incubated at room temperature for 10 min and transferred to a 48-well plate with 1 mL of culture medium. After 1 week in culture, the expanded cells were stained with anti-murine-TRBC-PE-Cy7 (RRID AB_893625) and anti-human-CD3-APC (RRID AB_1937212) and double positive cells were sorted using a BD FACSAria™ Fusion. Transfected Jurkat J76/CD8 stably expressing the respective E6 TCR (1×10^5 cells) were washed once with FACS buffer and stained with $E6_{18\text{-}26}$-HLA-A*02:01$^-$tetramers conjugated with APC. As a control for unspecific tetramer binding to the cells, we used PE-conjugated

HLA-A*02:01⁻tetramers loaded with CMV $pp65_{495\text{-}503}$ (irrelevant tetramer). Additionally, the cells were stained with anti-murine-TRBC-PECy7 (RRID AB_893625). After 30 min of incubation on ice, the cells were washed twice with FACS buffer, resuspended in FACS buffer and analyzed for multimer staining and murine-TRBC staining using a BD FACSCanto™ II flow cytometer. Dead cells were excluded by staining with DAPI at a concentration of 0.5 µg/mL. As negative controls non-transfected Jurkat J76/CD8 and Jurkat J76/CD8 expressing the CMV-reactive RA14 TCR (irrelevant TCR) [30] were also stained with $E6_{18\text{-}26}$-HLA-A*02:01-tetramers.

2.9 | Jurkat J76/CD8 activation assay upon Coculture with E6 peptide-loaded T2 cells

The T2 cell line was pre-loaded for 3 h with either $Insulin_{34\text{-}42}$ (1 µM, irrelevant peptide) or without peptide (NP) or with increasing concentrations of $E6_{18\text{-}26}$ peptide, ranging from 10^{-4} µM to 1 µM. The $Insulin_{34\text{-}42}$ is a well-known strong HLA-A2*02:01 binder used as a negative control to exclude any unspecific binding of the E6-TCR to HLA-A*02:01. After loading with peptide, the T2 cells were washed once with PBS and co-incubated with Jurkat J76/CD8 expressing the respective TCR (at 2:1 ratio) in 200 µL of RPMI with10% FBS for 18 h. Then, the mixed cell suspensions were retrieved, washed twice, resuspended in FACS buffer and stained for 20 min on ice with the following antibodies: anti-CD19-PE (RRID AB_2750097), anti-murine-TRBC-PECy7 (RRID AB_893625) and anti-CD69-APC (RRID AB_314845). Then, the cells were washed twice with FACS buffer and resuspended in 200 µL of FACS buffer. Flow cytometry analysis was performed in a BD FACSCanto™ II. Dead cells were excluded by staining with DAPI as described above. Expression of the CD69 activation marker was quantified in Jurkat cells (murine-TRBC⁺/CD19⁻). The results shown correspond to three independent experiments and are presented as mean ± standard deviation. Alternatively, T2 cells were loaded with either HPV16 $E6_{18\text{-}26}$ (wild type), $E6Q21H_{18\text{-}26}$, $E6Q21D_{18\text{-}26}$ (all peptides at 100 nM), or with no peptide (NP) for 3 h. Then, Coculture with the Jurkat J76/CD8 cell lines expressing the respective TCRs was carried out as above.

2.10 | Activation assay of jurkat J76/CD8-AC1 and J76/CD8-AC2 upon coculture with cancer cells with endogenous expression of the HPV16 E6 protein

Cervical cancer cell lines C33a, CaSki, SiHa (HLA-A*02:01+ or −) and HNSCC cell lines PCI-13 and UPCI-SCC-154 (HLA-A*02:01⁺) were seeded in 96-well plates (5×10^4 cells/well), and incubated overnight. Then, the medium was removed and replaced with 200 µL of medium containing $5{\times}10^5$ Jurkat J76/CD8 cells expressing either an irrelevant TCR (RA14) or either the AC1 TCR or the AC2 TCR. The Coculture was incubated for 18 h. Then, the cells were retrieved, washed twice, resuspended in FACS buffer and stained for 20 min on ice with anti-murine-TRBC-PECy7 and anti-CD69-APC antibodies. Next, the cells were washed twice with FACS buffer and, finally, resuspended in 200 µL of FACS buffer. Dead cells were excluded by staining with DAPI as described above. Flow cytometry analysis of the stained cells was performed in a BD FACSCanto™ II. Expression of the CD69 activation marker was quantified in murine-TRBC⁺ cells, of which, the CD69⁺ subpopulation was gated above the background seen with the SiHa and C33a negative controls. Alternatively, SiHa cells (HLA-A*02:01+ or −) were seeded in 96-well plates (5×10^4 cells/well) in 100 µL of DMEM with or without addition of interferon-gamma (IFN-γ, 50 ng/mL; Biolegend) and were incubated for 24 h. From that point and onwards, a coculture experiment with Jurkat J76/CD8 cells was carried as described above. The results shown correspond to three independent experiments and are presented as mean ± standard deviation.

2.11 | NK-92/CD3/CD8-derived cell lines with stable expression of an E6-reactive TCR

We described previously a NK-92-derived cell line with stable expression of the human CD3 and CD8 genes (NK-92/CD3/CD8).[13] For electroporation with plasmids carrying the respective TCRs, $1{\times}10^6$ NK-92 cells were washed twice with PBS and resuspended in 20 µL of Lonza P3 solution. Then, 1 µL of plasmid DNA mix containing 0.6 µg pSB-TCR and 0.4 µg/µL transposase plasmid were added to the suspension of cells and electroporation was performed with the Lonza 4D Nucleofector × instrument using the program EH115. After electroporation, the cells were incubated for 10 min at room temperature and subsequently retrieved with culture medium and transferred to a 48-well plate well with 1 mL of medium. After 2 weeks in culture, stable-transfectants were stained with anti-murine-TRBC-PE-Cy7 (RRID AB_893625) and anti-human-CD3-APC (RRID AB_1937212). Double positive cells were gated and sorted using a BD FACSAria™ Fusion.

2.12 | Cytotoxicity assays using live-cell imaging

Target cell lines with stable expression of the mWasabi fluorescent protein were seeded in 96 well plates (1.25×10^4 cells/well), and incubated overnight. Cells of the indicated NK-92- cell lines were washed twice with PBS and stained with the Tag-it Violet™ cell tracking dye (Biolegend) for 15 min at 37°C. Then, the NK-92 cells were washed twice with medium and resuspended in X-VIVO™20 with 5% FBS and propidium iodide (PI, Invitrogen; working concentration: 5 µg/mL) to a density of 2.5×10^4 cells/mL. To initiate the Coculture, the medium of the target cells was removed and replaced with the NK-92 cell suspension (effector-to-target 2:1) and incubated 15 min to allow the cells to settle down. Next, the live cell imaging time course experiment was started in a Zeiss Axio Observer Z1 motorized inverted fluorescence microscope. Pictures were taken hourly for 48 h, using the 10× objective lens, in the four channels: bright field, green (mWasabi), blue (labeled NK cells), and red (PI). Pictures were taken in the same fixed fields throughout the experiment. To quantify the number of dead cells in a time-resolved

manner, an image analysis protocol was made in CellProfiler™ (version 4.2.5).[31] It was adjusted for the transformation of color to gray-scale images, compatible with the software. Next, a module for the automatic recognition of PI^+ cells was implemented. As an output, the number of PI^+ cells per image and time point was obtained. For the representation of the data, the dead cell counts were normalized by subtracting the number of initial dead cells in each field (time 0), respectively. Alternatively, a second image analysis protocol was implemented by adding a module for the automatic recognition of the mWasabi$^+$ cells, for each image the number of target cells was quantified. For representation of the results, the number of mWasabi$^+$ target cells were normalized by dividing by the initial number of target cells (time 0).

Tumor spheroids were generated from UPCI-SCC-154-A2/mWasabi cells by seeding 2×10^4 cells per well in a 96 well Ultra-Low attachment plate (Corning) in DMEM supplemented with 10% fetal bovine serum (FBS, Gibco) and penicillin/streptomycin. The plate was centrifuged and incubated at 37°C/5% CO_2 for 48 h to allow spheroid formation. The NK cells were stained with the Tag-it Violet™ cell tracking dye, as described above. Then, the medium of each well was replaced with 150 µL of medium containing 5 µg/mL of propidium iodide, 50 µg/mL of Geltrex (Thermo Fischer Scientific) and 10^4 NK cells. The plate was preincubated in the microscope chamber for 45 min before starting a time course live cell imaging, taking Z-stack images hourly during 18 h in the green (mWasabi), blue (NK cells) and red (PI) channels using a 20× objective. Pictures were taken in the exact same position throughout the experiment, using a Zeiss Celldiscoverer seven automated confocal microscope and the ZEN 3.7 software (Carl Zeiss). Five spheroids and two optical slices (5-µm-thick) per condition were analyzed. As a measure of cell death, the integrated intensity of the PI^+ cells in the images was quantified using an image analysis pipeline created in CellProfiler.

2.13 | Analysis of expression of TCR costimulatory ligands by T2 cells

T2 cells (5×10^4 per sample) were washed twice with five volumes of FACS buffer and resuspended in 50 µL of the respective antibody (1 µg/mL, anti-human): CD86-APC (RRID AB_493232), CD80-PerCP-Cy5 (RRID AB_2566490), CD83-APC-Cy7 (RRID AB_2566392), CD70-PE (RRID AB_2561430), CD58-PE (RRID AB_1186063), OX40L-PE (RRID AB_2207272), CD137L-PE (RRID AB_314882), and ICOSL-PE (RRID AB_2280082). The cells were stained for 30 min on ice in the dark, washed twice with five volumes of FACS buffer and resuspended in 200 µL of FACS buffer with DAPI (0.5 µg/mL)and analyzed in a BD FACSCanto™ II.

2.14 | Cloning of human ICOSL in a sleeping beauty expression vector

Human primary CD8 T cells were isolated as already described. 0.5 × 10^6 of the isolated CD8 T cells were left activating in 1 mL of medium with 50 µL of TransAct™ for 3 days. Next, cells were collected and used for mRNA extraction using the RNeasy Mini Kit (Qiagen). The purified mRNA was used for reverse transcription using the RevertAid First Strand cDNA Synthesis Kit (1 h at 42°C) using the Oligo(dT)18 primer. The human ICOSL sequence was amplified from the cDNA of the activated CD8 T cells using the forward 5′–gcaccatgggactgg gcagtcctgga–3′ and reverse 5′–tccgtctagacgtggccagtgagctct–3′ primers (Sigma). The PCR reaction contained 25 µL of Phusion™ High Fidelity PCR Master Mix (2X) mixed with 2.5 µL of cDNA, 2.5 µL forward primer (10 µM), 2.5 µL reverse primer (10 µM) and 72.5 µL of PCR grade water. A two-step PCR cycling program was used as follows: 98°C/30 s, 35 cycles of [98°C/10 s; 72°C/15 s], ending with 72°C/5 min. Finally, the amplified ICOSL gene was cloned into the pSB bi-Pur plasmid.

2.15 | LDH cytotoxicity assay

The T2 cell line and its derivative cell line stably expressing ICOSL (T2/ICOSL) were pre-loaded for 3 h with either $CMVpp65_{495\text{-}503}$ (1 µM), $Insulin_{34\text{-}42}$ (1 µM, irrelevant peptide) or no peptide (NP) in X-VIVO™ 20. The T2 cells were then washed once with PBS and co-incubated for 18 h with NK-92/CD3/CD8/RA14 cells (100 000 T2:50 000 NK-92) in 200 µL of X-VIVO™20 with 5% FBS. Then, half of the medium from each well was transferred to a new 96-well U bottom plate, centrifuged to spin down any cells and debris and 50 µL of the supernatant were used to measure lactate dehydrogenase (LDH) activity using the Cytotoxicity Detection Kit PLUS (Roche). As controls, supernatants of T2 and NK-92 cells cultured separately were taken, and as 100% lysis control lysed T2 cells were used. The signal obtained for the medium-only control was subtracted from all conditions. Lysis was expressed as a percentage of the 100% lysis control of the respective T2 cells.

2.16 | Construction of an L1-CAR and expression in NK-92/CD3/CD8 cells

A gene was designed encoding a CAR against the L1CAM surface protein (denominated L1-CAR) with the following organization: The human CD8a signal peptide; a Myc tag; the scFv of a previously validated anti-L1CAM antibody,[32] the human CD28 hinge, transmembrane and intracellular domains of human ICOS. The construct was obtained as a synthetic gene and was cloned into the pSB plasmid. For the generation of cell lines expressing the L1-CAR, NK-92/CD3/CD8 and NK-92/CD3/CD8/AC1 were electroporated as described above. Shortly, 1×10^6 cells were washed twice with PBS and resuspended in 20 µL of Lonza P3 solution, then, 1 µL of plasmid DNA mix containing 0.6 µg transposon and 0.4 µg/µL transposase plasmids were added to the suspension of cells. After adding the plasmid mix, the cells were electroporated in the Lonza 4D Nucleofector × instrument using program EH115. After electroporation, the cells were incubated for 10 min at room temperature and subsequently retrieved with culture medium and transferred to a

48-well plate well with 1 mL of medium. After 2 weeks in culture, stable transfectants were detected by staining with anti-myc tag-AF647 (RRID AB_2888732) antibody. Three sequential sortings were performed to obtain populations with homogenous and stable expression of the L1-CAR. The cells were isolated by FACS in a BD FACSAria™ Fusion instrument.

For imaging flow cytometry analysis of the expression of the AC1-TCR and L1-CAR, NK-92 cell lines were stained as for conventional flow cytometry analysis and finally resuspended at a density of 10^7 cells/mL in FACS buffer with DAPI (0.5 µg/mL). Samples were then analyzed using an ImageStream®X Mark II. Single-cell pictures were taken for 10^3 single and fully stained samples. Image analysis was performed using Iluminex Ideas Software. For binding assays of soluble L1CAM protein by NK-92 cells expressing the L1-CAR, the cells were collected, washed with five volumes of FACS buffer, resuspended in FACS Buffer containing 1 µg/mL of recombinant L1CAM protein (Sino Biological) and incubated on ice for 30 min. The cells were then washed with ten volumes of FACS buffer and stained with anti-L1CAM-PE antibodies (RRID AB_2616787) for 30 min on ice. Finally, the cells were washed with 10 volumes of FACS buffer, and resuspended in FACS buffer containing DAPI (0.5 µg/mL) and analyzed in a BD FACSCanto™ II.

2.17 | Statistical analysis

Statistical analyses of the data between groups were performed using GraphPad Prism software v9 through a one-way ANOVA test, considering $p < 0.05$ as significant. Group means ± SD were plotted.

3 | RESULTS

3.1 | The HPV16 $E6_{18-26}$ peptide is predicted to be efficiently cleaved, transported to the ER, and loaded into HLA-A*0201 molecules

Previous studies using available prediction algorithms have identified a number of HLA class I-restricted HPV16 E6 peptides. Of these, only a few are HLA-A*02:01-restricted and have been clinically validated, most notably the $E6_{29-38}$ epitope.[10,33] Nevertheless, an E6-reactive TCR specific to the $E6_{29-38}$ epitope that was tested in a phase I clinical trial showed only two partial responses out of 12 treated patients.[11] Therefore, we sought here to identify new HPV16 E6-reactive TCRs to develop TCR-based therapies. To this end, we retrieved the amino acid sequence of the E6 protein from the Uniprot database (Accession number P03126) and used it as input in the Proteasomal cleavage/TAP transport/MHC class I combined predictor resource in the Immune Epitope Database and Analysis Resource (IEDB).[34] Only epitopes consisting of 9, 10, or 11 amino acids were considered. This algorithm integrates scores for predicted peptide cleavage by the proteasome, TAP processing and binding affinity to the respective HLA type, providing a combined score, which is directly proportional to the efficiency of epitope presentation. The top ten epitopes derived from the E6 protein displaying the highest combined score are summarized in Table 1. The HPV16 $E6_{18-26}$ peptide is predicted to be the most efficiently processed epitope, surpassing the rest of the epitopes in the individual MHC binding affinity, proteasome cleavage and TAP processing values and has the best combined score.

TABLE 1 Predicted HLA-A*02:01-restricted linear epitopes on the HPV16 E6 protein.

Aminoacids	Peptide	MHC prediction	TAP prediction	Cleavage prediction	Combined prediction
18–26	KLPQLCTEL	0.547	1.198	0.97537	0.79641
59–69	IVYRDGNPYAV	0.524	0.656	0.94482	0.75298
52–60	FAFRDLCIV	0.526	0.245	0.84575	0.72242
29–38	TIHDIILECV	0.508	0.462	0.81312	0.7025
28–38	TTIHDIILECV	0.377	0.292	0.81312	0.56725
59–68	IVYRDGNPYA	0.366	−0.194	0.78333	0.5374
125–135	HLDKKQRFHNI	0.357	0.419	0.56799	0.49527
97–106	QQYNKPLCDL	0.244	1.063	0.85422	0.46278
61–69	YRDGNPYAV	0.238	0.372	0.94482	0.45988
37–45	CVYCKQQLL	0.277	1.072	0.68506	0.45794

Note: The consensus amino acid sequence of HPV16 E6 was obtained from the UniProt database and introduced in the Proteasomal cleavage/TAP transport/MHC class I combined predictor tool in the Immune Epitope Database and Analysis Resource (IEDB) to identify HLAHLA-A*02:01-restricted-A*02:01-restricted epitopes. This algorithm predicts the binding affinity of the epitope to the MHC molecule, as well as the efficiency of transport by the TAP and cleavage by the proteasome. Finally, from the three individual scores, a combined score is calculated. The top ten epitopes with higher combined scores are displayed in descending order. The E618-26 epitope (highlighted in red) performed better in all categories.

3.2 | Identification of $E6_{18-26}$-TCRs from PBMCs of healthy donors

To isolate CD8 T cells recognizing $E6_{18-26}$-HLA-A*02:01, we established a protocol based on sequential sorting of cells binding $E6_{18-26}$-HLA-A*02:01 tetramers. We started isolating CD8 T cells from ten HLA-A*02:01 healthy donors using magnetic bead separation. These cells were stained with anti-CD3 and anti-CD8 antibodies and with two sets of $E6_{18-26}$-HLA-A*02:01 tetramers, one conjugated with PE and the other with APC. To discard false positive events due to unspecific tetramer binding, only double tetramer-positive events were sorted (Figure 1A). Typically, 1-2/10^5 CD8 T cells were stained with the $E6_{18-26}$ tetramers. After 2 weeks, a single-cell sorting was carried out on double-positive cells for $E6_{18-26}$-HLA-A*02:01 tetramers (Figure 1A). Single cell RT-PCR was applied to identify the TRAV and TRBV sequences and the complementarity determining region 3 (CDR3). From the sequencing results, we identified two clonotypes: AC1 (TRAV12-2/TRAJ12 paired with TRBV9/TRBJ2-2), and AC2 (TRAV24/TRAJ24 and TRBV29/TRBJ1-1/TRBD1) (Supporting Information S1: Table I).

Furthermore, we analyzed the frequencies of the complementarity-determining region 3 (CDR3) of the beta chains of AC1 and AC2 in a previously reported data set of TCR repertoires of healthy donors and cancer patients.[35] Interestingly, we found that the AC1 CDR3beta was present in the TCR repertoire of healthy individuals (3/88, 3.4%). We also found that this CDR3beta was present in the TCR repertoire of a group of cancer patients at higher frequency (6/70, 8.6%). It was remarkable that the patients in that study comprised head and neck, lung, melanoma and colorectal cancer. Of these, the head and neck cancer cases had three clonotypes with this CDR3beta (Supporting Information S1: Figure 1). This observations support that the AC1 belongs to the public shared repertoire and that PBMCs from healthy donors are a viable source for the identification of HPV16 E6 reactive TCRs.

We then constructed the AC1 and AC2 TCRs by cloning the gene fragments coding the *TRAV* and *TRBV* in a Sleeping Beauty (SB)-based vector for stable expression of murinized human TCRs in engineered immune cells. The beta and alpha chains were expressed as a single bicistronic gene separated by a GSG-T2A sequence. The human constant chains were replaced by their murine homologs to prevent mispairing when introduced in cells expressing endogenous TCR and also to promote CD3 binding, as the murine beta constant chains have higher affinity to human CD3 than the human TCR constant chains.[36] Finally, an extra cysteine was introduced in the alpha constant region (T48C) and in the beta constant region (S57C) to promote the formation of an extra disulfide bridge intended to further stabilize the complex (Figure 1B).

3.3 | Jurkat J76/CD8 cells stably expressing either AC1 or AC2 TCRs bind $E6_{18-26}$-HLA-A*02:01 tetramers and are specifically activated upon coculture with antigen-presenting cells loaded with $E6_{18-26}$ peptide

Initial functional tests of AC1 and AC2 were carried out with Jurkat J76/CD8 cells electroporated with the SB transposon system. The RA14 TCR, reactive to the CMV $pp65_{495-503}$ peptide was used as irrelevant control. The Jurkat J76/CD8 cell line is a derivative of the Jurkat E6.1 cell line, devoid of endogenous TCR expression, which prevents mispairing of TCR alpha and beta chains with endogenous homologs.[23] 1 week after electroporation, we sorted the stable transfectants gating $CD3^+$ and murine beta constant TCR^+ cells. The newly generated Jurkat J76/CD8 cell lines, Jurkat/CD8/AC1 and Jurkat/CD8/AC2 and Jurkat/CD8/RA14 (>95% expressing the respective TCR) were stained with $E6_{18-26}$-HLA-A*02:01-PE and CMV $pp65_{495-503}$-HLA-A*02:01-APC tetramers. Both Jurkat/AC1 and Jurkat/AC2 cell lines were able to bind $E6_{18-26}$-HLA-A*02:01 tetramers, but not the CMV tetramer (Figure 1C).

The functionality of the TCRs in the Jurkat J76/CD8 cell lines was first tested using T2 cells. T2 is a HLA-A*02:01 B-lymphoblastoid cell line deficient in the transporter associated with antigen processing (TAP), which makes the cells incapable of endogenous antigen processing and loading on HLA- A*02:01. However, T2 cells are still able to present exogenously administered peptides by stabilization of surface HLA-A*02:01. T2 cells were loaded with either no peptide (NP), an irrelevant peptide ($Insulin_{34-42}$ 1 μM), or decreasing concentrations of the HPV16 $E6_{18-26}$ (ranging from 10 pM to 1 μM) and separately cocultured overnight with the different Jurkat/TCR cell lines. Expression of CD69, a marker for T cell activation, was increased upon Coculture with T2 cells loaded with the $E6_{18-26}$ peptide (Figure 1D). With Jurkat/AC1, we detected a significant increase in surface CD69 at a peptide concentration of 0.1 μM, while Jurkat/AC2 activation was only detected at peptide concentration of 1 μM. These results confirm the specificity of the AC1 and AC2 TCRs towards the HPV16 $E6_{18-26}$ in the context of HLA-A*02:01 presentation, and suggests that AC1 has higher affinity and stronger functional capacity.

3.4 | Cervical cancer and HNSCC cell lines to study TCR-specific recognition of $E6_{18-26}$

Activation and cytotoxicity tests with immune cells expressing either the AC1 or AC2 TCR were carried out using the following target cell lines: (i) C33a, cervical cancer cell line HPV16−, HLA-A*02:01$^+$; (ii) CaSki, cervical cancer cell line HPV16$^+$, HLA-A*02:01$^+$; (iii) SiHa, cervical cancer cell line HPV16$^+$, HLA-A*02:01$^-$; (iv) PCI-13, HNSCC cell line HPV16$^-$, HLA-A*02:01$^+$; and (v) UPCI-SCC-154, HNSCC cell line HPV16$^+$, HLA-A*02:01$^-$ (Table 2). We first verified the sequence of the HPV16 *E6* gene in the HPV16$^+$ cell lines by reverse-transcription of mRNA and PCR amplification of *E6*. We found that CaSki cells express an E6 variant with two changes compared with the E6 protein from the Uniprot database, one leading to the replacement of the lysine in position 17 by a glycine (E6K17G) and the second one leading to substitution of leucine by valine in position 90 (E6L90V). E6 in SiHa cells differs in two amino acid positions, E6L90V and E6E120A. The UPCI-SCC-154 cells showed a single variation in E6Q21H (Table 2). Therefore, two variants (E6K17G and E6Q21H) could affect the presentation of the $E6_{18-26}$ epitope.

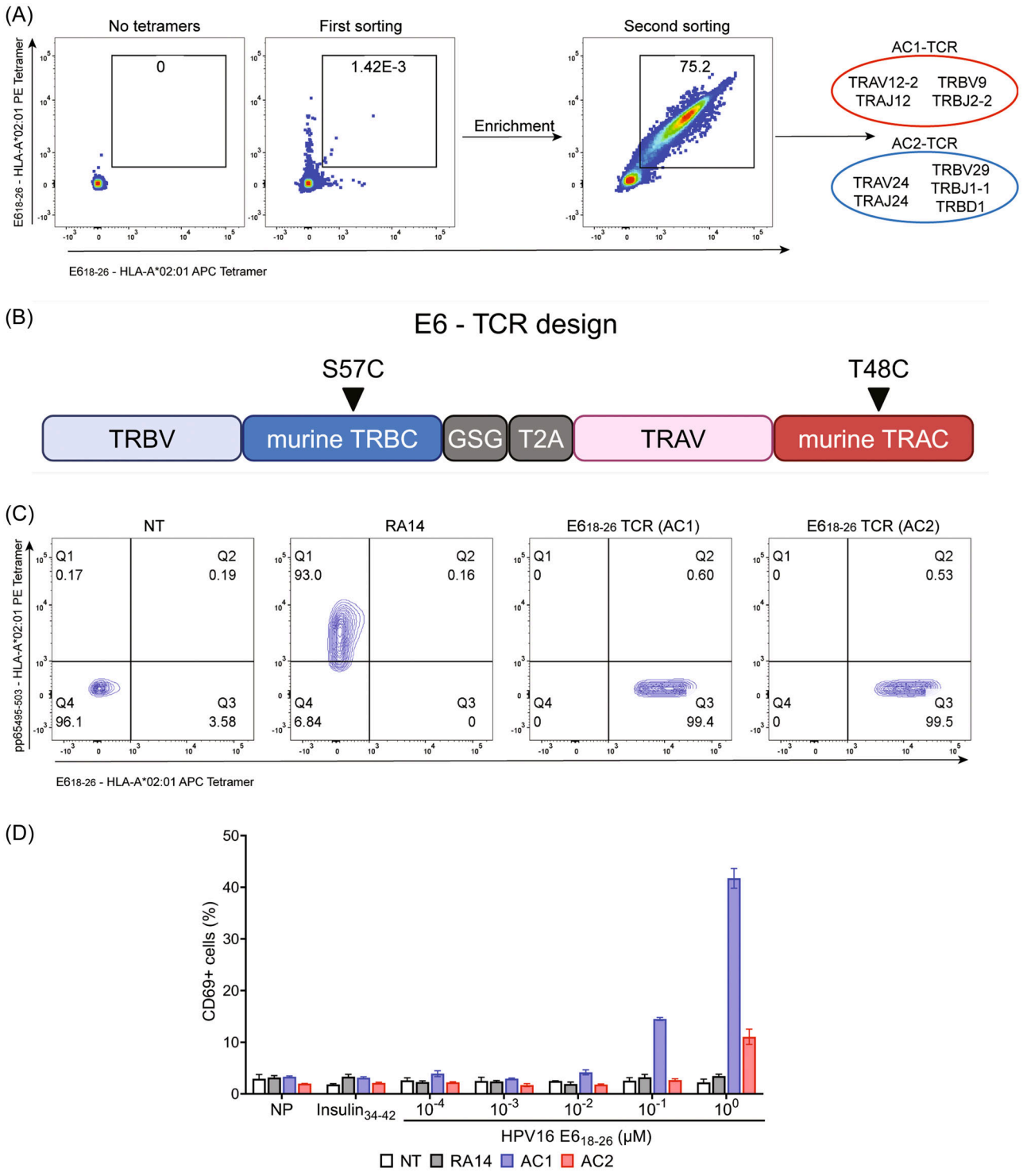

FIGURE 1 (See caption on next page).

3.5 | The HPV16 $E6_{18-26}$ peptide is presented in the context of HLA-A*02:01 by SiHa and UPCI-SCC-154 cells but not by CaSki cells

To determine whether the HPV16 $E6_{18-26}$ peptide is presented by the HPV16$^+$ cancer cell lines CaSki, SiHa/HLA-A*02:01 and, UPCI-SCC-154/HLA-A*02:01, Jurkat/AC1, Jurkat/AC2 and Jurkat/R14 (negative control) were co-incubated overnight with different target cells. Then, the Jurkat cells were retrieved and analyzed for surface expression of CD69. As negative target controls, we used the cervical cancer cell lines C33a (HPV$^-$, HLA-A*02:01$^+$), SiHa (parental line, HLA-A*02:01-) and the PCI-13 cell line (HPV16$^-$, HLA-A*02:01$^+$). We observed a clear and consistent activation of the Jurkat/AC1 upon Coculture with SiHa/HLA-A*02:01 (3.2% CD69$^+$ cells) and UPCI-SCC-154/HLA-A*02:01 cells (12.1% CD69$^+$ cells), above the background levels showed by the negative control (irrelevant TCR) (Figure 2A,B). In contrast, Jurkat/AC2 showed no activation.

We then tested whether enhancing antigen presentation by the target cells would lead to increase activation of Jurkat/AC1 cells co-incubated with SiHa/HLA-A*02:01$^+$ cells treated with IFNγ, which has been shown to increase HLA class I expression and induce a switch to the immunoproteasome.[37] The results showed nearly two-fold increase in the percentages of CD69$^+$ cells, while no change was observed in the negative controls (Figure 2C), which is consistent with augmented processing and presentation of the $E6_{18-26}$ peptide. Moreover, the strong activation of Jurkat/AC1 cells upon coculture with UPCI-SCC-154/HLA-A*02:01 cells, which express the E6Q21H variant, suggested that the $E6_{18-26}$Q21H peptide is indeed presented by HLA-A*02:01 and is recognized by the AC1 receptor. To further confirm this, we loaded T2 cells with either $E6_{18-26}$, $E6_{18-26}$Q21H, or $E6_{18-26}$Q21D peptides (Figure 2D). The latter was tested because it is identical to the HLA-A*02:01-restricted HPV18 $E6_{13-21}$ peptide, which means that, in case of cross-reactivity of the AC1 and/or AC2 TCRs with this peptide, they could be useful in a broader spectrum of HPV-caused cancers. The peptides were added to the T2 cells at a concentration of 0.1 μM and incubated for 3 h; T2 cells incubated with no peptide served as negative control. Overnight co-cultures with Jurkat/AC1, Jurkat/AC2s, or Jurkat/RA14 cells showed that the AC1 TCR reacted to the $E6_{18-26}$Q21H peptide (12.3% CD69$^+$ cells), in agreement with the reactivity of the Jurkat/AC1 cells towards the UPCI-SCC-154/HLA-A*02:01 cell line. In contrast, the Jurkat/AC2 did not react to $E6_{18-26}$Q21H, instead they showed some reactivity towards the $E6_{18-26}$Q21D peptide. These results support that the HPV16 $E6_{18-26}$ epitope is presented by SiHa/HLA-A*02:01$^+$ and UPCI-SCC-154/HLA-A*02:01$^+$ cells, but not by the parental SiHa or CaSki cells. Also, the data show cross-reactivity of the AC2 TCR to the $E6_{18-26}$Q21D peptide.

3.6 | Genetically engineered NK-92/CD3/CD8 cells expressing the AC1 TCR are capable of TCR-mediated cytotoxicity against SiHa/HLA-A*02:01 and UPCI-SCC-154/HLA-A*02:01 cells

We established previously a NK-92-derived cell line genetically modified to stably express the human CD3 and CD8 genes and showed its utility for in vitro characterization of recombinant TCRs.[13] To further investigate whether NK-92/CD3/CD8 cells expressing the AC1 TCR are capable of killing HPV16$^+$ tumor cells, we established a live-imaging cytotoxicity

TABLE 2 Relevant characteristics of the HPV16+ cell lines utilized in the study.

Cell line	C33a	CaSki	SiHa	PCI-13	UPCI-SCC-154
Origin	CC	CC	CC	HNSCC	HNSCC
HPV16	(−)	(+)	(+)	(−)	(+)
E6 mutation	—	K17G, L90V	L90V, E120A	—	Q21H

Note: Cervical cancer (CC) and head and neck cancer (HNSCC) cell lines used to test the functionality of the TCRs. The HPV16 negative cell lines C33a and PCI-13 were included as negative controls. The HPV16 E6 sequence was obtained by PCR amplification using as template cDNA synthesized from total RNA. Two missense mutations leading to single aminoacid substitutions were found.

FIGURE 1 Identification and characterization of TCRs reactive to the HPV16 $E6_{18-26}$-epitope. (A) CD8 T cells isolated from 10 donors were pooled and stained with anti-CD3, anti-CD8 and with two sets of HPV16 $E6_{18-26}$–HLA-A*02:01 tetramers: one conjugated with PE and another with APC. Double tetramer-positive CD3$^+$CD8$^+$ T cells were sorted and expanded for 2 weeks. Then, double tetramer-positive cells were sorted as single events in a 96-well PCR plate and used for single-cell TCR amplification and sequencing. Two clonotypes, named AC1 and AC2, were identified. (B) Schematic of the E6 TCR construct. (C) Transgenic Jurkat J76/CD8 cells stably expressing the indicated TCRs (>95% expression) were stained with APC-conjugated $E6_{18-26}$-HLA-A*02:01 tetramers or with an irrelevant tetramer (PE-conjugated CMV $pp65_{495-503}$-HLA-A*02:01 tetramers), as indicated. Jurkat J76/CD8 cells with no endogenous TCR (NT), and Jurkat J76/CD8 cells expressing the CMV-reactive RA14 TCR (irrelevant TCR) were used as negative and positive controls, respectively. (D) Dose-dependent activation of Jurkat J76/CD8 cell lines with stable expression of the indicated TCRs after Coculture with T2 cells loaded with increasing concentrations of the HPV16 $E6_{18-26}$ peptide. T2 cells were preincubated for 3 h with either no peptide (NP), $insulin_{34-42}$ (as control irrelevant peptide, 1 μM) or decimal increments of the HPV16 $E6_{18-26}$ peptide from 0.0001 μM to 1 μM. The T2 cells were then washed and cocultured with the respective Jurkat J76/CD8 cell line for 18 h. The cells were retrieved and stained with anti-CD19-PE, anti-murine TRBC-PECy7 and anti-CD69-APC. To exclude T2 cells, TRBC$^+$/CD19$^-$ cells were gated and analyzed for CD69 expression. Results from three independent experiments are shown as the mean ± standard deviation.

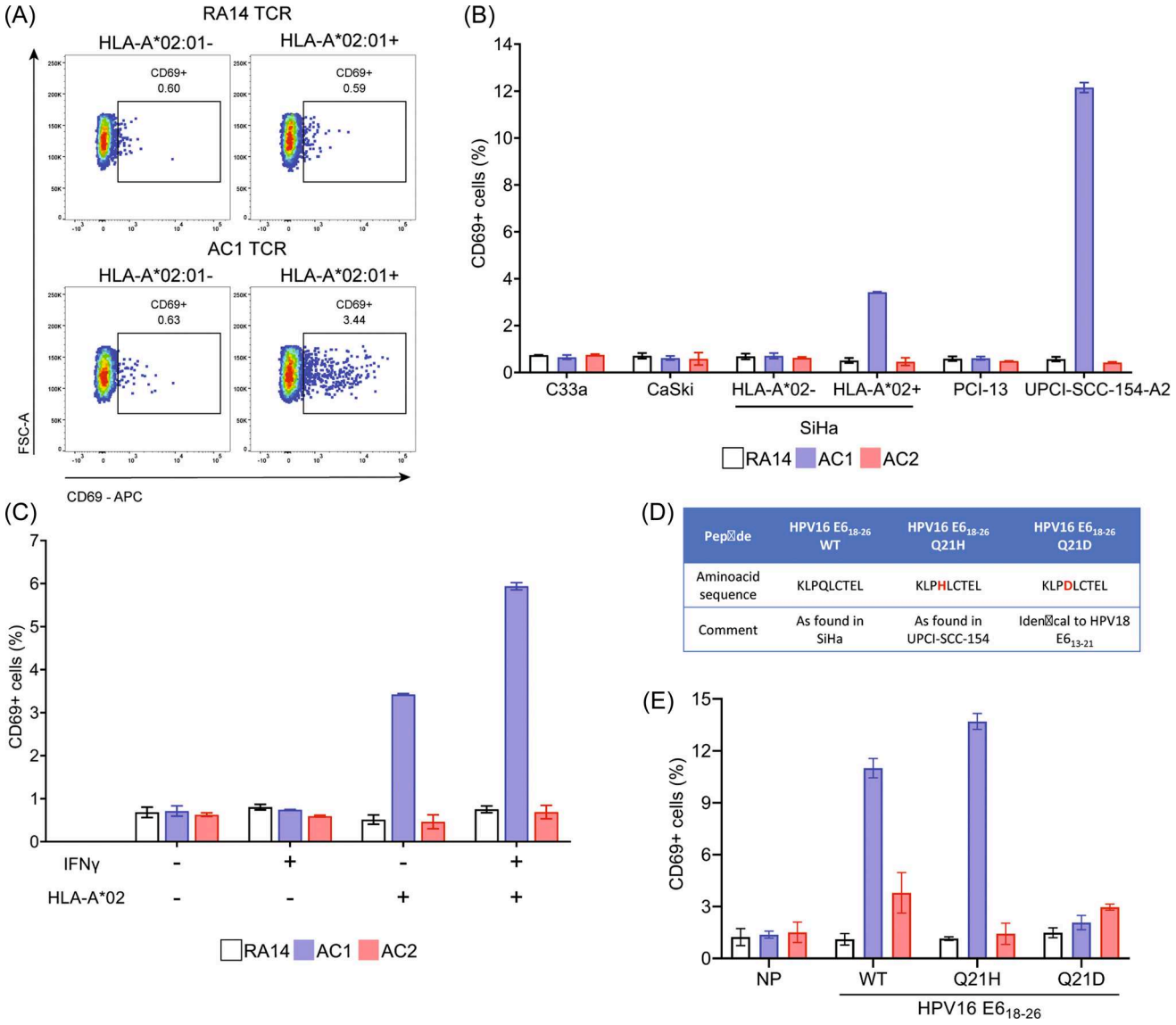

FIGURE 2 Activation of Jurkat J76/CD8 cells expressing AC1 or AC2 upon Coculture with HPV16$^+$ cancer cell lines. Jurkat J76/CD8 cell lines stably expressing the AC1, AC2 or RA14 TCR were cocultured for 18 h with the indicated cancer cell lines. Then, the Jurkat cells were retrieved and stained with anti-murine TRBC-PECy7 and anti-CD69-APC. (A) flow cytometry graphs showing the gating of CD69$^+$ Jurkat cells after co-incubation with SiHa cells HLA-A*02:01$^+$ or HLA-A*02:01$^-$. (B) Histogram representing the frequencies of CD69$^+$ Jurkat cells after co-incubation with the following cell lines: C33a (HPV16$^-$/HLA-A*02:01$^+$), CaSki (HPV16$^+$/HLA-A*02:01$^+$), SiHa (HPV16$^+$), SiHa-A2 (HPV16$^+$/HLA-A*02:01$^+$), PCI-13 (HPV16$^-$/HLA-A*02:01$^+$), and UPCI-SCC-154-A2 (HPV16$^+$/HLA-A*02:01$^+$). The percentage of CD69$^+$ Jurkat cells after Coculture with the respective cancer cell lines is shown as mean ± Standard deviation of three independent experiments. (C) SiHa/HLA-A*02:01$^+$ cells were stimulated with IFNγ (50 ng/mL) for 24 h before starting co-cultures with the Jurkat J76/CD8 cells expressing the indicated TCRs. The percentages of CD69$^+$ Jurkat cells after coculture in the presence or absence of IFNγ are shown as mean ± Standard deviation of three independent experiments. (D) Two E6 peptide variants used for further functional tests: HPV16 $E6_{18\text{-}26}$ containing the Q21H mutation that resembles the epitope potentially presented by the UPCI-SCC-154-A2 (HLA-A*02:01$^+$) cells; and $E6_{18\text{-}26}$ containing the Q21D mutation identical to the HPV18 $E6_{13\text{-}21}$ epitope, which is predicted to be presented by HPV18$^+$ cells (E) Activation of Jurkat J76/CD8 cells stably expressing the indicated TCRs after Coculture with T2 cells preincubated with no peptide (NP) or with either $E6_{18\text{-}26}$ peptide variant (0.1 μM). After loading the T2 cells for 3 h, the cells were washed and cocultured with the Jurkat J76/CD8 cell lines for 18 h. Afterwards, the cells were retrieved and stained with anti-CD19-PE, anti-murine TRBC-PECy7 and anti-CD69-APC. T2 cells were excluded by gating murine-TRBC$^+$/CD19$^-$. Results from three independent experiments are shown as the mean ± standard deviation.

method based on fluorescence microscopy to monitor target cell dead in a time resolved manner. First, we generated cancer cell lines with stable expression of the mWasabi fluorescent protein using the SB transposon system. These cell lines were sorted based on homogenous green fluorescence. To discriminate between target tumor cells and NK-92 cells, the latter were stained using a violet cell tracking dye (Tag-it Violet™). Then, co-cultures were started with NK-92/CD3/CD8 cells expressing the AC1 or an irrelevant TCR. Propidium iodide (PI) was added to the

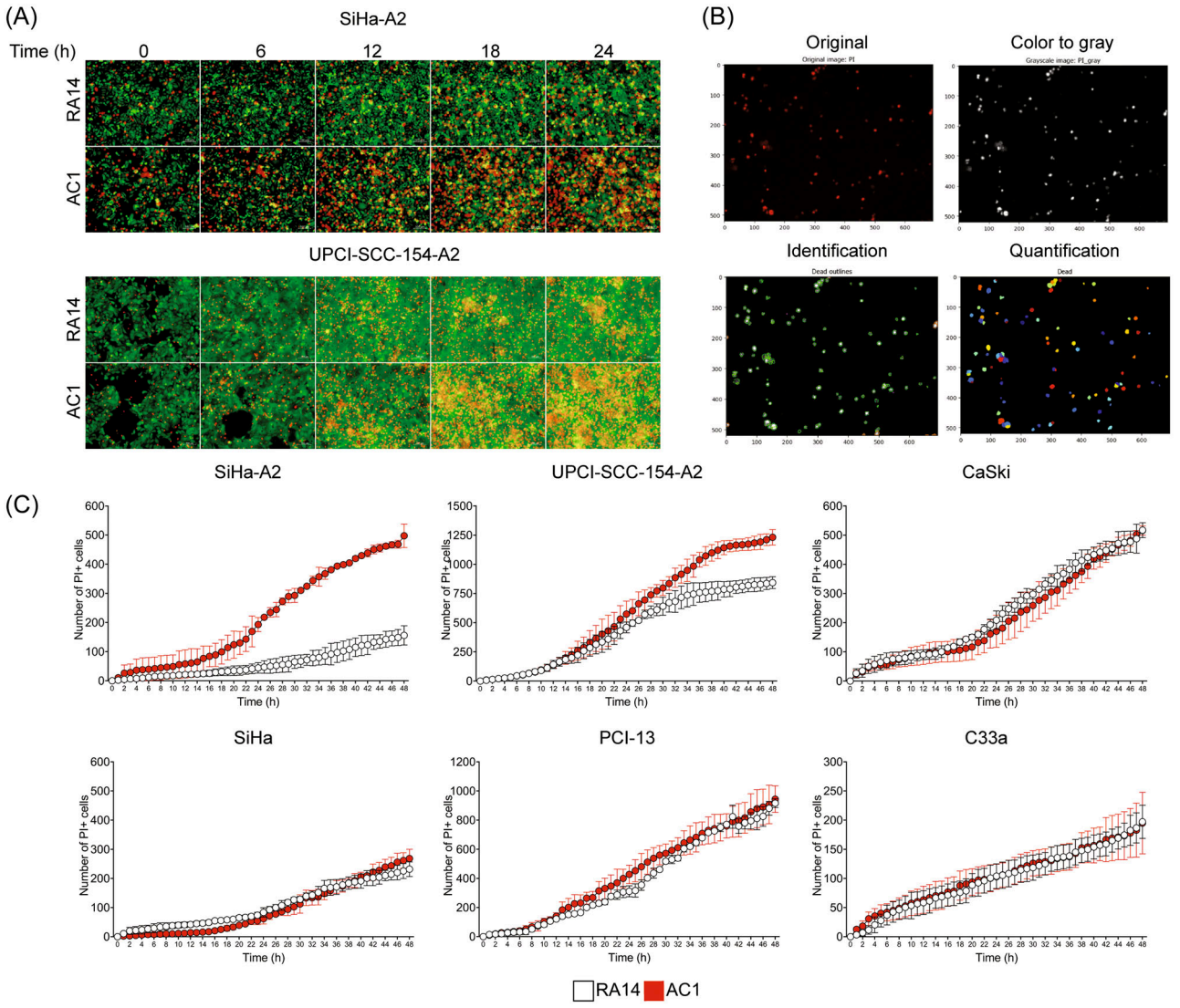

FIGURE 3 Detection and quantification of TCR-specific cytotoxicity of NK-92/CD3/CD8 cells expressing the AC1 receptor. (A) SiHa cells and SiHa-A2 cells expressing the mWasabi fluorescent protein were cocultured with NK-92/CD3/CD8-AC1 cells or NK-92/CD3/CD8-RA14 cells (irrelevant TCR) at a 2:1 (effector:target) ratio. The cells were stained with a violet proliferation dye and propidium iodide (PI) was incorporated into the coculture medium to monitor cell death along the incubation time in a live-cell imaging microscope equipped with a 5% CO_2°C and 37°C incubator. Pictures in the red (PI), violet (NK cells) and green (SiHa cells) channels were taken every hour for 48 h using a 10× objective. Representative images taken at the indicated time points are shown. (B) An image analysis pipeline was implemented for the identification and quantification of the PI^+ cells using the CellProfiler software. First, original images were converted to gray scale; subsequently, primary objects (PI^+ nuclei) were identified and counted per image. (C) Three independent experiments were conducted to quantify the number of dead cells arising during the coculture. The number of PI^+ cells obtained in the first picture were deducted from the rest of the pictures of the same 10× field. The same live-imaging cytotoxicity experiment was carried out with the C33a, CaSki, PCI-13 and UPCI-SCC-154-A2. Throughout, results of three independent experiments are represented as the mean ± standard deviation.

culture medium to detect dead cells, as the dying cells allow PI enter and bind nucleic acids thereby emitting red fluorescence. AC1 was selected considering the lack of activation of Jurkat J76/CD8/AC2 cells cocultured with the target cell lines in previous experiments (Figure 2B). To validate the method, we started with co-cultures of SiHa and SiHa/HLA-A*02:01 with NK-92/CD3/CD8/AC1 and NK-92/CD3/CD8/RA14 cells taking pictures hourly in the bright field, violet, green and red fluorescent channels at the same position over the course of 48 h. Coculture of SiHa/HLA-A*02:01$^+$ cells with NK-92/CD3/CD8/AC1 cells caused a significant increase in the number of PI^+ cells over the course of the experiment as compared with the NK-92/CD3/CD8/RA14 cells expressing the irrelevant TCR (Figure 3A). To quantify the numbers of dead cells per picture, we designed an image analysis pipeline using the CellProfiler software by first converting the images to grayscale and implementing a module for the identification of PI^+ cells, distinguishing fluorescent events based on their intensity, shape, and size (Figure 3B).

After 20 h of coculture, we found significantly higher numbers of PI^+ SiHa/HLA-A*02:01 cells cocultured with NK-92/CD3/CD8/AC1 cells

than with NK-92/CD3/CD8/RA14 cells, and the difference became progressively more pronounced until the end of the experiment. Meanwhile, no significant difference was observed with the parental SiHa cells (HLA-A*02:01-) (Figure 3C). Following the same protocol, we analyzed the cytotoxicity of the NK-92/CD3/CD8/AC1 cells towards the other cervical cancer and HNSCC cell lines. Of these, only co-cultures with UPCI-SCC-154/HLA-A*02:01 cells showed a significant increase in the numbers of PI^+ cells over time, starting at about 28 h. However, we did not detect significant cytotoxicity against CaSki cells, which is consistent with the results obtained with Jurkat J76/CD8/AC1 cells (Figure 2B). As expected, the C33a and PCI-13 cell lines (both HPV−) showed no significant cytotoxicity. These results are in agreement with the activation results obtained with the Jurkat J76/CD8 cells expressing the AC1 receptor and demonstrate the specific cytotoxicity of the NK-92/CD3/CD8/AC1 cells against the HLA-A*02:01$^+$ cell lines. They also suggest that CaSki cells do not present the $E6_{18\text{-}26}$ epitope.

3.7 | Design and construction of a L1-CAM ssdCAR

Previous reports suggested that the signaling induced by TCR engagement might not suffice to trigger effective activation of the immune cells and cytotoxicity against the target cells, likely due to low antigen presentation.[38–41] Thus, the expression of relevant costimulatory signals might be of critical importance to ensure proper activation of the immune cells. We analyzed the expression of a series of ligands of costimulatory receptors by T2 cells and found significant levels of CD80, CD86, CD83, CD70, and CD58 but only very low levels of ICOSL (Supporting Information S1: Figure 2). It has been shown that ICOS signaling is a strong costimulatory signal for T cells and is required for the proper functionality of activated T cells.[42] Further, ICOS stimulation has been shown to augment T cell [43] and NK functionality.[44,45] To test whether concomitant activation of ICOS signaling in NK-92/CD3/CD8 cells expressing a TCR could enhance TCR-mediated cytotoxicity, we first generated a T2-derived cell line constitutively expressing ICOSL (Figure 4A). Furthermore, the expression of ICOS in the effector NK-92/CD3/CD8 cells was confirmed by staining with an ICOS-specific antibody.

Then, we investigated the effect of ICOS stimulation on activation and cytotoxicity of NK-92/CD3/CD8/RA14 TCR upon TCR engagement were cocultured with T2 and T2/ICOSL cells, which were previously loaded either with CMV $pp65_{495\text{-}503}$, $insulin_{34\text{-}42}$ (irrelevant control) peptides or incubated likewise without peptide (NP). After 18 h of coculture, the supernatants were collected and analyzed for cell dead by measuring LDH activity. We found that ICOS stimulation led to a significantly higher specific cytotoxicity without increasing unspecific killing of T2/ICOSL cells that were not loaded with peptide or loaded with the irrelevant peptide (Figure 4B).

Having shown that ICOS stimulation enhances TCR-mediated cytotoxicity, we designed an ssdCAR against L1CAM (Supporting Information S1: Table II), a tumor-associated antigen overexpressed in a variety of cancers including HPV16-associated cancers and correlates with metastases and poor prognosis.[19,46,47] Furthermore, except for the C33a cell line, the rest of the cervical and HNSCC cell lines showed varying degrees of L1CAM expression (Supporting Information S1: Figure 3). Then L1-CAR carries the ICOS costimulatory intracellular domain, but is devoid of CD3ζ domain, in addition it carries a myc-tag that facilitates its detection (Figure 4C). The interaction of the L1-CAR with the L1CAM protein on HPV16$^+$ cancer cells offers the potential to enhance the TCR-specific cytotoxicity of the NK-92 cells, without undesired cytotoxicity against healthy cells expressing physiological levels of L1CAM (Figure 4D).

We introduced the L1-CAR into the NK-92/CD3/CD8 and also in its derivative cell line expressing the NK-92/CD3/CD8/AC1 using the SB system. We generated four cell lines with either no expression, individual expression of TCR or CAR, and co-expression of both (Figure 4E). Then, the TCR and CAR distribution on the surface of the cells was detected with anti-myc and anti-murine beta TCR constant antibodies and registered using an imaging flow cytometer. Both AC1-TCR and L1-CAR were found to be distributed scattered on the surface of the NK-92/CD3/CD8/AC1/L1-CAR cells, with abundant co-localization of both proteins (Figure 4F). To confirm that the L1-CAR can bind efficiently the L1CAM protein, we incubated NK-92/CD3/CD8/L1-CAR cells with recombinant soluble L1CAM protein and, after washing the unbound L1CAM, the cells were stained with an anti L1CAM antibody (different clonotype than that of the L1-CAR). The NK-92/CD3/CD8/AC1, NK-92/CD3/CD8/RA14 cells were used as negative controls. Only NK-92/CD3/CD8/L1-CAR cells were able to bind L1CAM (Figure 4G).

3.8 | NK-92/CD3/CD8 cells expressing both AC1 TCR and L1-CAR show enhanced cytotoxic capacity selectively against HPV16 E6$^+$ and L1CAM$^+$ cancer cell lines

The functionality and cytotoxic capacity of the dual receptor cell line NK-92/CD3/CD8/AC1/L1-CAR was tested by live-cell imaging fluorescence microscopy experiments using as target the two cell lines SiHa/HLA-A*02:01/mWasabi and UPCI-SCC-154/HLA-A*02:01/mWasabi. The target cells were cocultured for 24 h with the NK-92/CD3/CD8/AC1/L1-CAR cell line, and compared with the NK-92/CD3/CD8/AC1, the NK-92/CD3/CD8/L1-CAR and the NK-92/CD3/CD8/RA14 cell lines. A strong reduction in the numbers of UPCI-SCC-154 target cells was observed upon co-incubation with the dual AC1/L1-CAR cells starting after 7 h, with an evident increase in the number of PI+ cells, especially in the periphery of target cell isles (Figure 5A,B, UPCI-SCC-154-A2). The SiHa cells showed significant increases in the numbers of PI^+ cells from 8 h of co-incubation; however, the cytotoxic effect was consistent but somehow slower and required a longer co-incubation period (48 h) until almost all cells were eliminated (Figure 5A and B, SiHa-A2), leaving behind clumps of PI^+ cells and very few mWasabi$^+$ SiHa cells at the end of the coculture (Figure 5A, SiHa-A2). We also implemented a second image analysis pipeline for quantification of the numbers of target cells (mWasabi$^+$ cells) per field, normalizing the numbers of target cells to the initial numbers for each set (Supporting

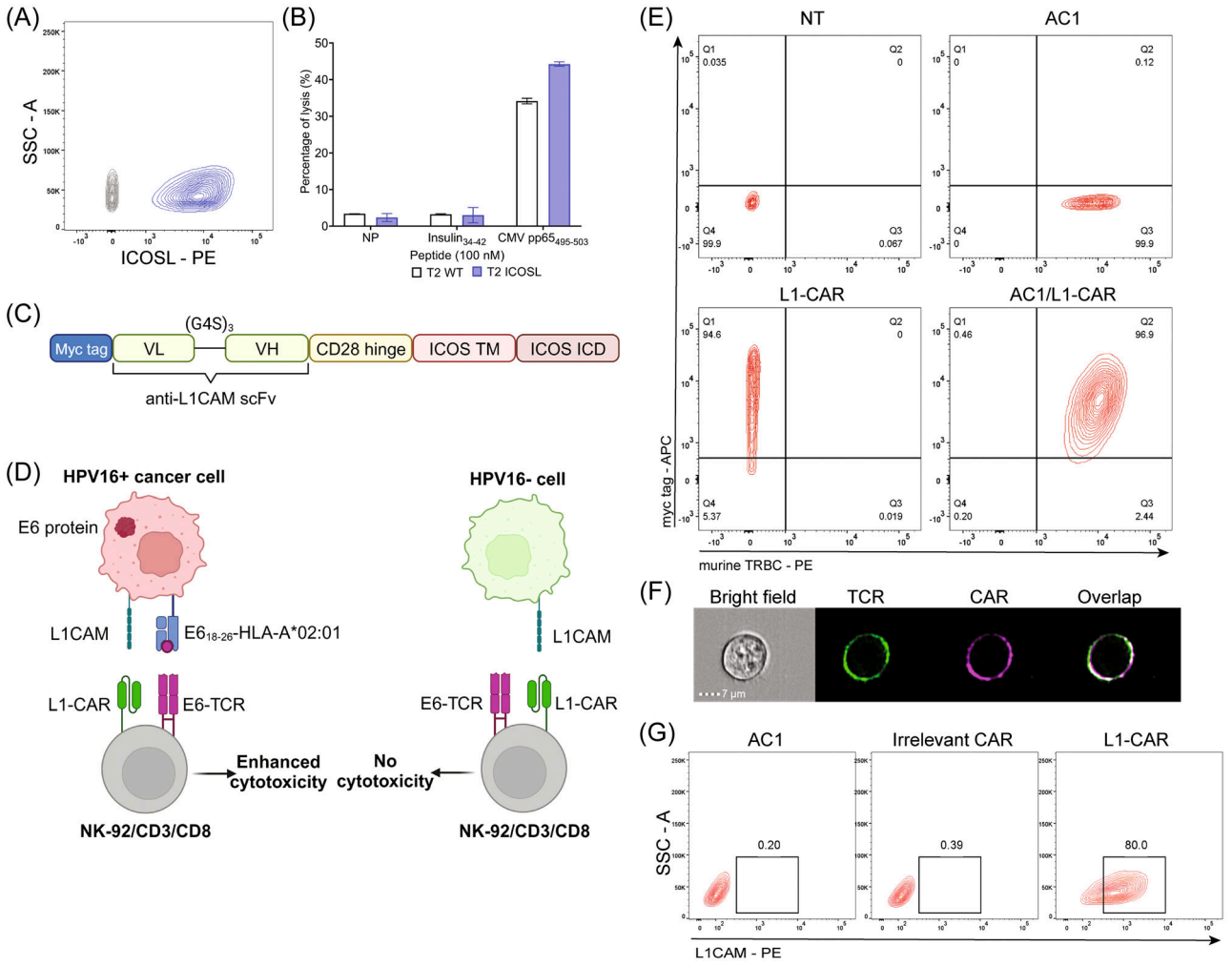

FIGURE 4 Generation of a NK-92/CD3/CD8 cell line co-expressing a costimulatory L1-CAR and a TCR reactive HPV16 $E6_{18-26}$. (A) Chromatogram of the transgenic T2 cell line constitutively expressing the human ICOSL that was generated by transfection using the Sleeping Beauty system. (B) Validation of the T2-ICOSL cell line for TCR cytotoxicity tests. T2 and T2-ICOSL cells were loaded with either CMV $pp65_{495-503}$ peptide (100 µM), with $insulin_{34-42}$ (irrelevant, 100 µM) or incubated without peptide (NP) for 3 h and later on co-incubated with NK-92/CD3/CD8/RA14 cells at a ratio of 1:2 (effector:target ratio) for 18 h. Then, the supernatants were collected and analyzed for LDH activity to determine the percentage of lysed T2 cells resulting of the co-incubation. As controls, NK cells alone, T2 cells alone, lysates of T2 cells (control 100% lysis) and culture medium (background control) were processed in parallel. (C) Schematic representation of the anti-L1CAM ssdCAR (L1-CAR) constructed for this study. VH and VL: variable domains of the heavy and light chains, TM: transmembrane domain, ICD: intracellular domain. (D) Cartoon showing the combination of the AC1-TCR with the costimulatory L1-CAR in the NK-92/CD3/CD8 cells. Cytotoxicity is expected only against HPV16 infected cells presenting the $E6_{18-16}$ peptide in the context of HLA-A*02:01 which additionally express L1CAM, leading to enhanced avidity and signaling strength ($HPV16^+$ cancer cell). The signaling triggered by the L1-CAR alone is not sufficient to elicit a cytotoxic response towards cells not presenting the $E6_{18-16}$ peptide ($HPV16^-$ cell). (E) Expression of AC1-TCR and L1-CAR in NK-92/CD3/CD8 cell lines stably expressing each receptor separately (AC1-TCR, L1-CAR) or both (AC1-TCR/L1-CAR). The latter cell line was generated by stable transfection of an L1-CAR expression vector into cells expressing the AC1 TCR. The cells were stained with anti-murine TRBC-PE, and anti-Myc tag-AF647 antibodies. (F) Surface appearance of the AC1-TCR and L1-CAR on NK-92/CD3/CD8/AC1/L1-CAR cells stained with anti-murine TRBC-PE and anti-Myc tag-AF647 antibodies and analyzed using an imaging flow cytometer. Representative images are shown in the bright field, PE (577/35) and AF647 (702/85) channels. (G) Specific binding of soluble L1CAM protein by NK-92/CD3/CD8/L1-CAR cells. The cells were incubated with soluble L1CAM protein (1 µg/mL), washed and stained with an anti-L1CAM-PE antibody to detect L1CAM protein bound by the cells. As negative controls, non-transfected NK-92/CD3/CD8 cells and NK-92/CD3/CD8 expressing an irrelevant CAR (against TROP2) were simultaneously processed likewise.

Information S1: Figure 4A). This quantification further confirmed the strong cytolytic activity effect of the NK-92/CD3/CD8/AC1/L1-CAR cells against the UPCI-SCC-154-A2 cells (Supporting Information S1: Figure 4B).

We also tested the cytotoxicity of the NK-92/CD3/CD8/AC1/L1-CAR cells on UPCI-SCC-154-A2 cells in a 3-dimensional (3-D) setting, which offers less immediate direct effector-target cell contact than the 2-D system. To this end, we generated spheroids

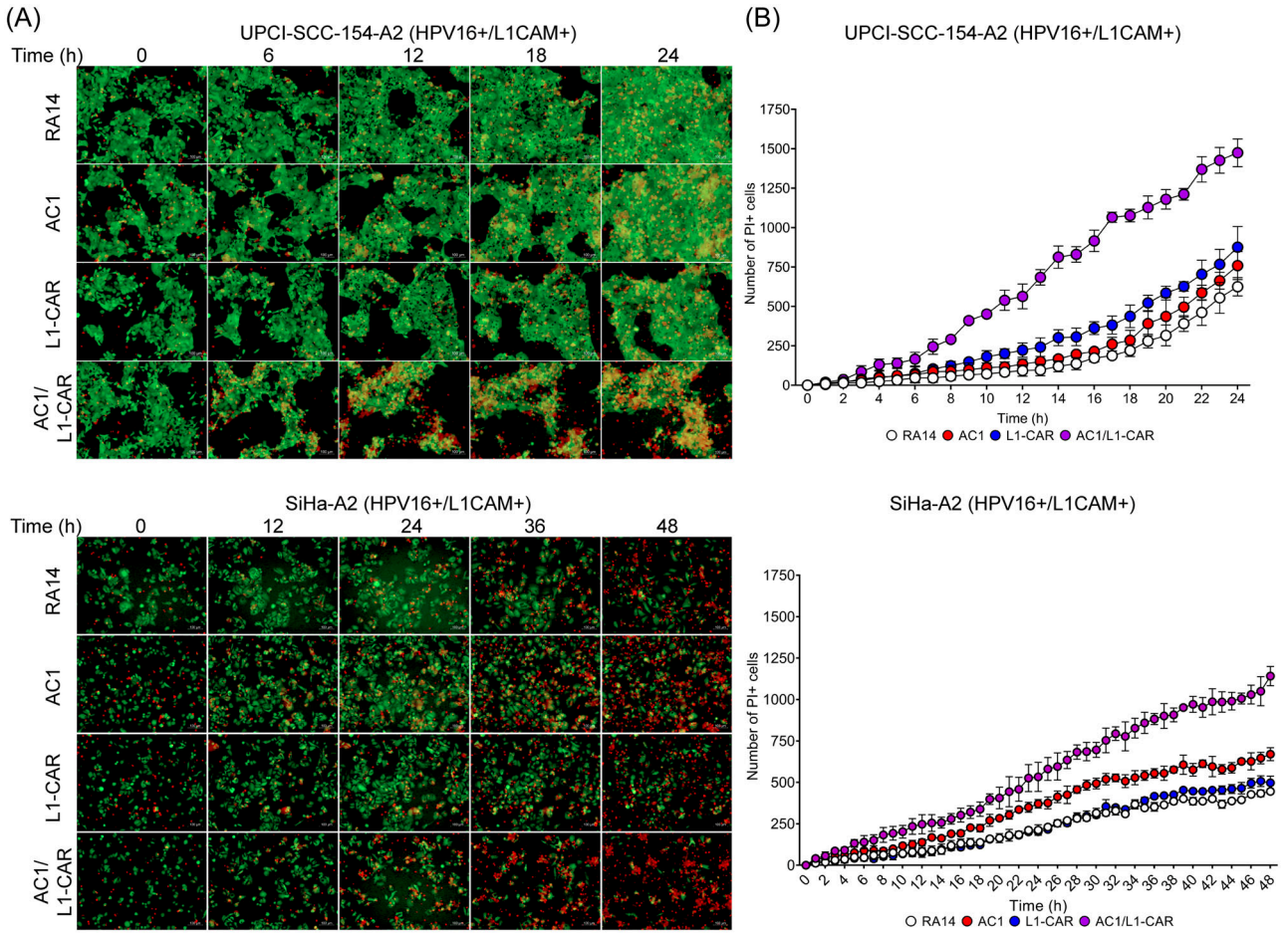

FIGURE 5 Synergistic effect of AC1 and L1-CAR in NK-92/CD3/CD8/AC1/L1-CAR cells co-incubated with HPV16$^+$/L1CAM$^+$ cancer cell lines. (A) Live fluorescence microscopy of NK-92/CD3/CD8 cells expressing either receptor (AC1-TCR or L1-CAR), both (AC1-TCR/L1-CAR) or the RA14-TCR (Irrelevant TCR). The NK-92/CD3/CD8 cells were stained with a violet proliferation dye and added to growing UPCI-SCC-154-A2 cells (mWasabi$^+$/HLA-A*02:01$^+$/HPV16$^+$/L1CAM$^+$) and to SiHa-A2 cells (mWasabi$^+$/HLA-A*02:01$^+$/HPV16$^+$/L1CAM$^+$). The effector:target ratio was 2:1. Propidium iodide was added to the culture medium to detect the dead cells. The coculture was monitored with a live-cell imaging microscope with the incubator set to 5% CO_2 and 37°C. Pictures in the red (PI, dead cells), violet (effector cells) and green (target cells) channels were taken hourly during either 24 h (UPCI-SCC-154-A2) or 48 h (SiHa-A2) using a 10× objective. Representative images of the green/red (merge) channels are shown for the indicated time points. The experiment was repeated three times and triplicates were run in parallel. (B) Quantification of the numbers of PI$^+$ cells along with the co-cultures. An image analysis pipeline was implemented using the CellProfiler software for the identification and quantification of the number of PI$^+$ cells. For each well, the values were normalized by subtracting the number of PI$^+$ cells at time zero. Results of three independent experiments are shown as the mean ± standard deviation.

with the UPCI-SCC-154-A2 cell line and co-incubated them with the different NK-92 cell lines, taking confocal fluorescence microscopy images in a time resolved manner and measuring the intensity of PI fluorescence in the images. After 18 h of coculture, we observed an significant increase in the intensity of PI fluorescence in the spheroids co-incubated with the dual AC1/L1-CAR cells compared with the controls (AC1, L1-CAR and RA14). Some PI$^+$ aggregates were seen within the spheroids in some of the images (Figure 6A). Moreover, the spheroids co-incubated with the dual cells were smaller. Quantification of the integrated intensity of PI fluorescence in the images confirmed a significant increase in intensity starting after 7 h of coculture, in agreement with the findings of the 2-D cytotoxicity experiment (Figure 6B). Taken together, these results demonstrate clear enhancement of the cytotoxic potential by the dual AC1/L1-CAR against HPV16$^+$ cancer cell lines expressing L1CAM.

4 | DISCUSSION

Immunotherapy of tumors caused by HPV16 is showing promising results in diverse modes.[48,49] Adoptive transfer of tumor infiltrating lymphocytes or TCR-engineered T cells targeting E6 or E7 have produced encouraging clinical results.[11,50] Nonetheless, critical limitations still need to be addressed, such as low affinity and avidity of engineered effector cells and weak signaling strength of tumor-reactive TCRs, which can lead to dysfunctionality.[51] In the present study, we aimed at identifying novel TCRs that recognize the HPV16

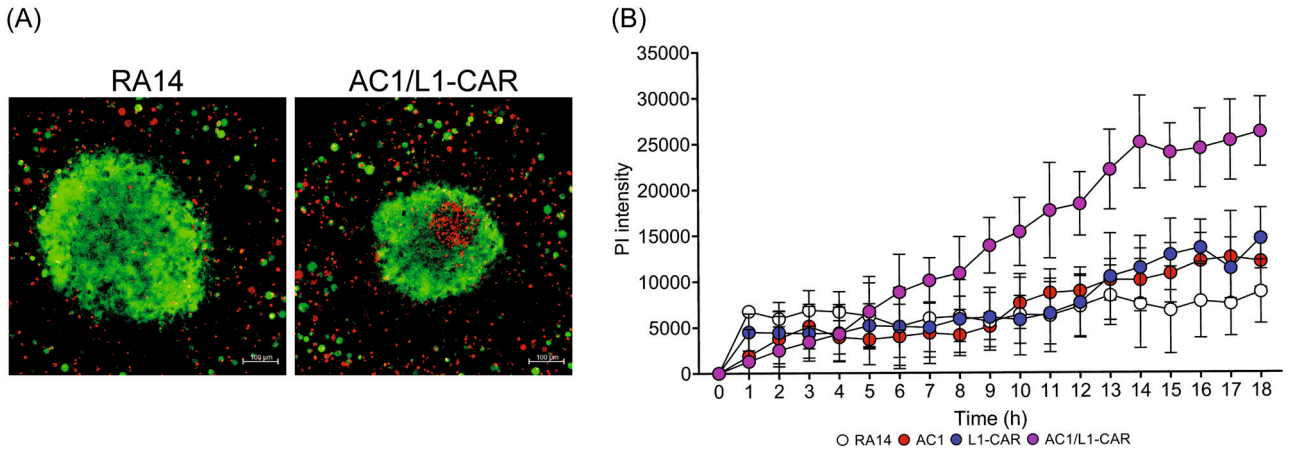

FIGURE 6 Synergistic effect of AC1 and L1-CAR in NK-92/CD3/CD8/AC1/L1-CAR cells co-incubated with spheroids of UPCI-SCC-154-A2 cells. Live confocal fluorescence microscopy of NK-92/CD3/CD8 cells expressing either receptor (AC1-TCR or L1-CAR), both (AC1-TCR/L1-CAR) or the RA14-TCR (irrelevant TCR). The NK-92/CD3/CD8 were stained with a violet proliferation dye and added to UPCI-SCC-154-A2 (mWasabi+/HLA-A*02:01+/HPV16+/L1CAM+) spheroids. Propidium iodide was added to the culture medium to detect the dead cells. The coculture was monitored with a confocal live-cell imaging microscope with the incubator set to 5% CO_2 and 37°C. Pictures in the red (PI^+, dead cells), violet (effector cells) and green (target cells) channels were taken hourly during 18 h using a 20× objective. (A) Representative images of the same stack showing the green/red (merge) channels for the NK-92/CD3/CD8/RA14 and NK-92/CD3/CD8/AC1/L1-CAR cell lines after 18 h of co-incubation. The experiment was repeated three times and triplicates were run in parallel. (B) Quantification of the integrated intensity of PI^+ cells throughout the co-cultures. An image analysis pipeline was implemented using the CellProfiler software for the quantification of the integrated intensity of PI fluorescence per image. For each well, the values were normalized by subtracting the integrated intensity at time zero. Results of three independent experiments are shown as the mean ± standard deviation.

$E6_{18\text{-}26}$ epitope, which has not been explored before. Besides, it was intended to enhance the TCR signaling strength by co-expression, in the same effector cell, of a TCR and an ssdCAR targeting L1CAM, a protein frequently overexpressed in $HPV16^+$ tumors. The main goal was to enhance the cytotoxic response against tumor cells while reducing on-target off-tumor toxicity.

Epitope prediction algorithms predict for the HPV16 $E6_{18\text{-}26}$ epitope the highest HLA-A*02:01 binding, TAP processing, and proteasome cleavage scores (Table 1). Indeed, the $E6_{18\text{-}26}$ epitope was the first E6 epitope identified as HLA-A*02:01-restricted peptide from a cancer cell line expressing the HPV16 E6 protein.[8] Moreover, high avidity CD8 T cells reactive to $E6_{18\text{-}26}$ were reported in the peripheral blood, lymph nodes and tumors of patients.[52] Yet, immunopeptidomics analyses of a $HPV16^+$ cancer cell line failed to detect it, but the mass spectrometry signal was close to the limit of detection, suggesting that it was overlooked due to technical limitations.

Another HPV16 E6 relevant CD8+ T cell epitope is the $E6_{29\text{-}38}$ peptide. A TCR that recognizes this epitope was identified previously and tested in a phase I/II clinical trial.[11] Unfortunately, this epitope comprises a mutation hotspot within the E6 gene inducing changes in the epitope conformation[12] in a way that might hinder its recognition by the TCR, which could explain the limited success of the clinical study. This highlights the importance of identifying new TCRs against other HPV16 antigens, such as the $E6_{18\text{-}26}$ epitope, which could translate into a more efficient immunotherapy.

Here, we have developed and standardized quick protocol based on double peptide-HLA multimer staining and sequential cell sorting with which we were able to identify two $E6_{18\text{-}26}$-reactive TCRs (AC1 and AC2) from pools of CD8 T cells of multiple healthy donors (Figure 1). We demonstrate that this method allows the isolation and sequencing of neoantigen-specific TCRs from CD8 T cells of healthy donors in less than 2 weeks, which is faster than methods relying on stimulation of PBMCs with antigen-presenting cells that typically take about 4 weeks.[53] To our knowledge, this study is the first reporting the identification of TCRs from peripheral blood $CD8^+$ T cells of healthy individuals, which are specific to the $E6_{18\text{-}26}$ peptide naturally presented in the context of HLA-A*02:01. The fact that the CDR3beta of AC1was present in the TCR repertoire of healthy individuals and cancer patients at relatively high frequencies suggests that it is public shared repertoire and supports the usefulness of PBMCs from healthy donors for the identification of neoepitope-reactive TCRs. Likewise, we are currently using circulating $CD8^+$ T cells of healthy donors to identify TCRs that recognize nonviral neoantigens (Quiros-Fernandez and Cid-Arregui, unpublished).

Jurkat/AC1 and Jurkat/AC2 cells were shown comparably labeled with [$E6_{18\text{-}26}$–HLA-A*02:01] tetramers and both cell lines were activated after co-incubation with T2 cells loaded with $E6_{18\text{-}26}$ peptide, indicating that both receptors are functional. Activation was evidenced at the highest peptide concentrations tested (0.1-1 μM; Figure 1). This suggests a moderate binding affinity of the $E6_{18\text{-}26}$ peptide to HLA-A*02:01, as shown previously.[9] Jurkat/AC1 became activated when cocultured with two different cancer cell lines $HPV16^+$/HLA-$A*02:01^+$, which is an indirect proof of natural $E6_{18\text{-}26}$ presentation. This results contradict a previous report suggesting that the $E6_{18\text{-}26}$ peptide was not presented in the context of

HLA-A*02:01 on HPV16$^+$ cell lines.[9] However, it might well be that the E6$_{18\text{-}26}$ was missed at that time. MS-based immunopeptidomics is an evolving field and its sensitivity is continuously improving.[54] Jurkat/AC2 cells did not show significant activation, which is consistent with the results obtained with peptide-loaded T2 cells, in which the Jurkat/AC2 cells showed low activation and only at higher peptide concentrations performing objectively worse than Jurkat/AC1. Pre-stimulation of the SiHa/HLA-A*02:01 cells with IFNγ to enhance antigen processing and presentation consistently increased the activation of Jurkat/AC1 cells, demonstrating dose-dependent engagement of the AC1 TCR with endogenously processed and presented E6 in SiHa cells.

Surprisingly, Jurkat/AC1 cells cocultured with CaSki cells did not show activation, despite being HPV16$^+$ and HLA-A*02:01$^+$. E6 mRNA sequencing confirmed that, unlike the other cell lines tested in this study (Table 2), CaSki cells express a variant E6 coding a glycine at position 17 instead of lysine (K17G),[55] compared with the HPV16 reference sequence. We speculate that this change might hinder the processing and presentation of the E6$_{18\text{-}26}$ peptide. Indeed, this peptide was not detected using a very sensitive method based on LC-MS^3 detection of HLA-presented peptides on CaSki cells.[56] The UPCI-SCC-154 cells express a Q21H E6 variant inside the E6$_{18\text{-}26}$ epitope. However, this cell line elicited high activation of the Jurkat/AC1 cells. Tests with T2 cells confirmed the high affinity of the AC1 TCR by the E6$_{18\text{-}26}$ Q21H peptide (Figure 2). The Jurkat/AC1 cells were not activated by the E6$_{18\text{-}26}$ Q21D peptide (identical to HPV18 E6$_{13\text{-}21}$), while the AC2 TCR showed low but significant reactivity.

We used a derivative of the NK-92 cell line (NK-92/CD3/CD8) that allows functional characterization of newly identified TCRs [13] to analyze the cytotoxic capacity of NK-92/CD3/CD8/AC1 cells against HPV16$^+$ tumor cell lines in live-cell imaging experiments in a time resolved manner. The NK-92/CD3/CD8/AC1 cells specific cytotoxic activity against SiHa/HLA-A*02:01 and UPCI-SCC-154-A2 cells, but not against parental SiHa (HLA-A*02:01-), CaSki cells or PCI-13 and C33A (both HPV16-) (Figure 3). A time dependent increase in the number of PI$^+$ target cells was also observed for the NK-92/RA14 cells (irrelevant TCR control), which could be expected due to the intrinsic antitumoral cytotoxicity of this cell line. These results are in agreement with the activation results obtained with Jurkat/AC1, providing further proof of the processing and presentation of the HPV16E6$_{18\text{-}26}$ epitope by HPV16$^+$ cancer cells and demonstrating that the AC1 TCR is fully functional.

We have previously demonstrated that simultaneous expression of a TCR recognizing the well-characterized E7$_{11\text{-}19}$ epitope of HPV16 E7 and a costimulatory TROP-2 CAR in the same effector cell (NK-92 or T cells) significantly enhances its cytotoxic capacity.[13] However, the TROP-2 CAR carried two intracellular signaling domains (CD28 and 41BB) and, despite its demonstrated synergism with the TCR, the TROP-2 CAR still induced moderate standalone activation of the effector cells, causing cytotoxicity towards cells expressing high levels of TROP-2 even in the absence of E7 expression. In the present study, we constructed the L1-CAR with ICOS as single intracellular signaling domain and devoid of CD3ζ domain. The aim was to reduce standalone activity of the L1-CAR, thus improving the tumor cell-specificity of this combinatorial approach. L1CAM has been found to be a strong predictor for recurrence of tumors and decreased survival,[19] and is associated with more aggressive cervical tumors.[21] With our approach, we envisioned to enhance the functionality of NK-92/CD3/CD8/AC1 cells by means of costimulation with the L1CAM CAR. Activation and cytotoxic activity of NK-92/CD3/CD8/AC1/L1-CAR cells would occur only after both AC1 TCR and L1-CAR engage simultaneously their respective targets in HPV16$^+$/L1CAM$^+$ cancer cell lines. Imaging flow cytometry analysis showed that the AC1 TCR and the L1-CAR colocalized and were evenly distributed, on the surface of the cells and live-cell imaging cytotoxicity experiments demonstrated synergism between both receptors in 2-D and 3-D settings. In both, the combination of TCR and CAR was highly cytotoxic to the target cells compared with that observed when the receptors were expressed separately.

Altogether, our results demonstrate that the HPV16 E6$_{18\text{-}26}$ epitope is processed and presented by HLA-A*02:01 molecules on cervical and oropharyngeal cancer cells and, hence, is an attractive target for adoptive cell therapies. Further, we have validated the functionality and cytotoxic capacity of a newly identified TCR that recognizes the E6$_{18\text{-}26}$ epitope and have demonstrated the synergistic effect of this TCR and an L1CAM ssdCAR with lower stand-alone cytotoxicity, which is expected to overcome the risk of on-target, off-tumor toxicity. The selection pressure exerted by the immune system against HPV16+ tumor cells induces the generation of different escape variants of the E6 gene, which might coexist even within the same tumor contributing to intra-tumor heterogeneity. Thus, new approaches need to be developed, for instance combining an ssdCAR with different TCRs each reactive against a specific epitope (e.g., E6$_{18\text{-}26}$, E6$_{29\text{-}38}$, E7$_{11\text{-}19}$) that might provide a higher coverage against the different tumor cell subpopulations and hence an improved efficacy of the immunotherapy. Although not having an animal model to test the TCR/CAR engineered NK cells could be a limitation of this study, we intend to initiate a clinical trial, as it has been done previously.[10]

AUTHOR CONTRIBUTIONS

Isaac Quiros-Fernandez contributed to study design, conducted experimental work, data analysis, interpretation and representation, and wrote the manuscript. Sofia Libório-Ramos, Lena Leifert and Bruno Schönfelder conducted experimental work and analyzed results. Israel Vlodavsky, validation, writing review and editing. Angel Cid-Arregui conceived the idea, designed the project, conducted experimental work, interpreted the results and wrote the manuscript. Isaac Quiros-Fernandez, Sofia Libório-Ramos, Lena Leifert, Bruno Schönfelder, Israel Vlodavsky and Angel Cid-Arregui verified the data. All authors had full access to all the data in the study and approved the final version of the manuscript.

ACKNOWLEDGMENTS

IQF was supported by the University of Costa Rica and the German DAAD. This work was supported in part by the Cooperation Program in Cancer Research of the Deutsches Krebsforschungszentrum

(DKFZ) and Israel's Ministry of Science, Technology and Space (MOST). We thank Elisa Arias, Angela Diez and Kevin Delgado for technical assistance. We are grateful to the Flow Cytometry, Microscopy and Peptide Synthesis Core Facilities at DKFZ. ACA dedicates this study to the memory of Prof. Harald zur Hausen, who laid the foundation for understanding the HPV causality of cancer. His continuous advice and support are gratefully acknowledged. He passed away on May 29, 2023. Open Access funding enabled and organized by Projekt DEAL.

CONFLICT OF INTEREST STATEMENT

The authors declare no conflict of interest.

DATA AVAILABILITY STATEMENT

The raw data of this study are deposited in the database of the German Cancer Research Center (DKFZ), and can be provided to inquiers upon reasonable requests. The data that support the findings of this study are available from the corresponding author upon reasonable request.

ORCID

Angel Cid-Arregui http://orcid.org/0000-0003-1433-2922

REFERENCES

1. Baulu E, Gardet C, Chuvin N, Depil S. TCR-engineered T cell therapy in solid tumors: state of the art and perspectives. *Sci Adv*. 2023;9(7):eadf3700.
2. Chandran SS, Klebanoff CA. T cell receptor-based cancer immunotherapy: emerging efficacy and pathways of resistance. *Immunol Rev*. 2019;290(1):127-147.
3. Vats A, Trejo-Cerro O, Thomas M, Banks L. Human papillomavirus E6 and E7: what remains? *Tumour Virus Res*. 2021;11:200213.
4. Alhamlan FS, Alfageeh MB, Al Mushait MA, Al-Badawi IA, Al-Ahdal MN. Human papillomavirus-associated cancers. *Adv Exp Med Biol*. 2021;1313:1-14.
5. McBride AA. Oncogenic human papillomaviruses. *Philos Trans R Soc, B*. 2017;372(1732):20160273.
6. Butz K, Ristriani T, Hengstermann A, Denk C, Scheffner M, Hoppe-Seyler F. siRNA targeting of the viral E6 oncogene efficiently kills human papillomavirus-positive cancer cells. *Oncogene*. 2003;22(38):5938-5945.
7. Yoshinouchi M, Yamada T, Kizaki M, et al. In vitro and in vivo growth suppression of human papillomavirus 16-positive cervical cancer cells by E6 siRNA. *Mol Ther*. 2003;8(5):762-768.
8. Bartholomew JS, Stacey SN, Coles B, Burt DJ, Arrand JR, Stern PL. Identification of a naturally processed HLA A0201-restricted viral peptide from cells expressing human papillomavirus type 16 E6 oncoprotein. *Eur J Immunol*. 1994;24(12):3175-3179.
9. Riemer AB, Keskin DB, Zhang G, et al. A conserved E7-derived cytotoxic T lymphocyte epitope expressed on human papillomavirus 16-transformed HLA-A2+ epithelial cancers. *J Biol Chem*. 2010;285(38):29608-29622.
10. Draper LM, Kwong MLM, Gros A, et al. Targeting of HPV-16+ epithelial cancer cells by TCR gene engineered T cells directed against E6. *Clin Cancer Res*. 2015;21(19):4431-4439.
11. Doran SL, Stevanović S, Adhikary S, et al. T-cell receptor gene therapy for human papillomavirus-associated epithelial cancers: a first-in-human, phase I/II study. *J Clin Oncol*. 2019;37(30):2759-2768.
12. Ai W, Wu C, Jia L, et al. Deep sequencing of HPV16 E6 region reveals unique mutation pattern of HPV16 and predicts cervical cancer. *Microbiol Spect*. 2022;10(4):e0140122.
13. Poorebrahim M, Quiros-Fernandez I, Marmé F, Burdach SE, Cid-Arregui A. A costimulatory chimeric antigen receptor targeting TROP2 enhances the cytotoxicity of NK cells expressing a T cell receptor reactive to human papillomavirus type 16 E7. *Cancer Lett*. 2023;566:216242.
14. Crossin KL, Krushel LA. Cellular signaling by neural cell adhesion molecules of the immunoglobulin superfamily. *Dev Dyn*. 2000;218(2):260-279.
15. Fogel M, Gutwein P, Mechtersheimer S, et al. L1 expression as a predictor of progression and survival in patients with uterine and ovarian carcinomas. *Lancet*. 2003;362(9387):869-875.
16. Chen D, Zeng Z, Yang J, et al. L1cam promotes tumor progression and metastasis and is an independent unfavorable prognostic factor in gastric cancer. *J Hematol Oncol*. 2013;6:43.
17. Boo YJ, Park JM, Kim J, et al. L1 expression as a marker for poor prognosis, tumor progression, and short survival in patients with colorectal cancer. *Ann Surg Oncol*. 2007;14(5):1703-1711.
18. Allory Y, Matsuoka Y, Bazille C, Christensen EI, Ronco P, Debiec H. The L1 cell adhesion molecule is induced in renal cancer cells and correlates with metastasis in clear cell carcinomas. *Clin Cancer Res*. 2005;11(3):1190-1197.
19. Schrevel M, Corver WE, Vegter ME, et al. L1 cell adhesion molecule (L1CAM) is a strong predictor for locoregional recurrences in cervical cancer. *Oncotarget*. 2017;8(50):87568-87581.
20. Kim JH, Lee KW, Ahn DG, Oh KY, Yoon HJ. Clinical significance of L1CAM expression and its biological role in the progression of oral squamous cell carcinoma. *Oncol Rep*. 2023;49(4):67.
21. Mancusi de Carvalho JP, Salim RC, Carvalho FM, Nogueira Dias Genta ML, Baracat EC, Carvalho JP. L1 cell adhesion molecule (L1CAM) in stage IB cervical cancer: distinct expression in squamous cell carcinomas and adenocarcinomas. *J Clin Pathol*. 2020;73(11):748-753.
22. Stranzl T, Larsen MV, Lundegaard C, Nielsen M. NetCTLpan: pan-specific MHC class I pathway epitope predictions. *Immunogenetics*. 2010;62(6):357-368.
23. Heemskerk MHM, Hoogeboom M, de Paus RA, et al. Redirection of antileukemic reactivity of peripheral T lymphocytes using gene transfer of minor histocompatibility antigen HA-2-specific T-cell receptor complexes expressing a conserved alpha joining region. *Blood*. 2003;102(10):3530-3540.
24. Salter RD, Howell DN, Cresswell P. Genes regulating HLA class I antigen expression in T-B lymphoblast hybrids. *Immunogenetics*. 1985;21(3):235-246.
25. Tam YK, Maki G, Miyagawa B, Hennemann B, Tonn T, Klingemann HG. Characterization of genetically altered, interleukin 2-independent natural killer cell lines suitable for adoptive cellular immunotherapy. *Hum Gene Ther*. 1999;10(8):1359-1373.
26. Ai H, Olenych SG, Wong P, Davidson MW, Campbell RE. Hue-shifted monomeric variants of clavularia cyan fluorescent protein: identification of the molecular determinants of color and applications in fluorescence imaging. *BMC Biol*. 2008;6:13.
27. Giudicelli V, Brochet X, Lefranc MP. IMGT/V-QUEST: IMGT standardized analysis of the immunoglobulin (IG) and T cell receptor (TR) nucleotide sequences. *Cold Spring Harbor Protocols*. 2011;2011(6):pdb.prot5633.
28. Kowarz E, Löscher D, Marschalek R. Optimized sleeping beauty transposons rapidly generate stable transgenic cell lines. *Biotechnol J*. 2015;10(4):647-653.
29. Rosskopf S, Leitner J, Paster W, et al. A Jurkat 76 based triple parameter reporter system to evaluate TCR functions and adoptive T cell strategies. *Oncotarget*. 2018;9(25):17608-17619.
30. Wagner EK, Qerqez AN, Stevens CA, Nguyen AW, Delidakis G, Maynard JA. Human cytomegalovirus-specific T-cell receptor engineered for high affinity and soluble expression using mammalian cell display. *J Biol Chem*. 2019;294(15):5790-5804.

31. Stirling DR, Swain-Bowden MJ, Lucas AM, Carpenter AE, Cimini BA, Goodman A. CellProfiler 4: improvements in speed, utility and usability. *BMC Bioinformatics*. 2021;22(1):433.
32. Wolterink S, Moldenhauer G, Fogel M, et al. Therapeutic antibodies to human L1CAM: functional characterization and application in a mouse model for ovarian carcinoma. *Cancer Res*. 2010;70(6):2504-2515.
33. Santegoets SJ, Welters MJP, Schrikkema DS, et al. The common HLA class I-restricted tumor-infiltrating T cell response in HPV16-induced cancer. *Cancer Immunol Immunother*. 2023;72(6):1553-1565.
34. Tenzer S, Peters B, Bulik S, et al. Modeling the MHC class I pathway by combining predictions of proteasomal cleavage, TAP transport and MHC class I binding. *CMLS Cell Mol Life Sci*. 2005;62(9):1025-1037.
35. immunoSEQ hsTCRB-V4b Control Data [Internet]. 2020 [cited 22/02/2024]. Available from: http://adaptivebiotech.com/pub/tcrbv4-control
36. Cohen CJ, Zhao Y, Zheng Z, Rosenberg SA, Morgan RA. Enhanced antitumor activity of murine-human hybrid T-cell receptor (TCR) in human lymphocytes is associated with improved pairing and TCR/CD3 stability. *Cancer Res*. 2006;66(17):8878-8886.
37. Zhou F. Molecular mechanisms of IFN-γ to up-regulate MHC class I antigen processing and presentation. *Int Rev Immunol*. 2009;28(3-4):239-260.
38. Dhatchinamoorthy K, Colbert JD, Rock KL. Cancer immune evasion through loss of MHC class I antigen presentation. *Front Immunol*. 2021;12:636568.
39. González PA, Carreño LJ, Coombs D, et al. T cell receptor binding kinetics required for T cell activation depend on the density of cognate ligand on the antigen-presenting cell. *Proc Nat Acad Sci*. 2005;102(13):4824-4829.
40. Engels B, Engelhard VH, Sidney J, et al. Relapse or eradication of cancer is predicted by peptide-major histocompatibility complex affinity. *Cancer Cell*. 2013;23(4):516-526.
41. Deeg J, Axmann M, Matic J, et al. T cell activation is determined by the number of presented antigens. *Nano Lett*. 2013;13(11):5619-5626.
42. Lownik JC, Conrad DH, Martin RK. T cell receptor signaling defines the fate and pathway of ICOS internalization. *Biochem Biophys Rep*. 2020;24:100803.
43. Wyatt MM, Huff LW, Nelson MH, et al. Augmenting TCR signal strength and ICOS costimulation results in metabolically fit and therapeutically potent human CAR Th17 cells. *Mol Ther*. 2023;31(7):2120-2131.
44. Ogasawara K, Yoshinaga SK, Lanier LL. Inducible costimulator costimulates cytotoxic activity and IFN-γ production in activated murine NK cells. *J Immunol*. 2002;169(7):3676-3685.
45. Montes-Casado M, Ojeda G, Aragoneses-Fenoll L, et al. ICOS deficiency hampers the homeostasis, development and function of NK cells. *PLoS One*. 2019;14(7):e0219449.
46. Altevogt P, Doberstein K, Fogel M. L1CAM in human cancer. *Int J Cancer*. 2016;138(7):1565-1576.
47. Maten MV, Reijnen C, Pijnenborg JMA, Zegers MM. L1 cell adhesion molecule in cancer, a systematic review on domain-specific functions. *Int J Mol Sci*. 2019;20(17):4180.
48. Fakhr E, Modic Ž, Cid-Arregui A. Recent developments in immunotherapy of cancers caused by human papillomaviruses. *Immunology*. 2021;163(1):33-45.
49. Norberg SM, Hinrichs CS. Engineered T cell therapy for viral and non-viral epithelial cancers. *Cancer Cell*. 2023;41(1):58-69.
50. Nagarsheth NB, Norberg SM, Sinkoe AL, et al. TCR-engineered T cells targeting E7 for patients with metastatic HPV-associated epithelial cancers. *Nat Med*. 2021;27(3):419-425.
51. Shakiba M, Zumbo P, Espinosa-Carrasco G, et al. TCR signal strength defines distinct mechanisms of T cell dysfunction and cancer evasion. *J Exp Med*. 2022;219(2). doi:10.1084/jem.20201966
52. Zehbe I, Kaufmann AM, Schmidt M, Hohn H, Maeurer MJ. Human papillomavirus 16 E6-specific CD45RA+ CCR7+ high avidity CD8+ T cells fail to control tumor growth despite Interferon-γ production in patients with cervical cancer. *J Immunother*. 2007;30(5):523-532.
53. Montes M, Rufer N, Appay V, et al. Optimum in vitro expansion of human antigen-specific CD8 T cells for adoptive transfer therapy. *Clin Exp Immunol*. 2005;142(2):292-302.
54. Yewdell JW. MHC class I immunopeptidome: past, present, and future. *Mol Cell Proteomics*. 2022;21(7):100230.
55. Meissner JD. Nucleotide sequences and further characterization of human papillomavirus DNA present in the CaSki, SiHa and HeLa cervical carcinoma cell lines. *J Gen Virol*. 1999;80(Pt 7):1725-1733.
56. Blatnik R, Mohan N, Bonsack M, et al. A targeted LC-MS strategy for low-abundant HLA class-I-presented peptide detection identifies novel human papillomavirus T-cell epitopes. *Proteomics*. 2018;18(11):e1700390.

SUPPORTING INFORMATION

Additional supporting information can be found online in the Supporting Information section at the end of this article.

How to cite this article: Quiros-Fernandez I, Libório-Ramos S, Leifert L, Schönfelder B, Vlodavsky I, Cid-Arregui A. Dual T cell receptor/chimeric antigen receptor engineered NK-92 cells targeting the HPV16 E6 oncoprotein and the tumor-associated antigen L1CAM exhibit enhanced cytotoxicity and specificity against tumor cells. *J Med Virol*. 2024;96:e29630. doi:10.1002/jmv.29630